Galerkin Method for Nonlinear Dynamics

Bernd R. Noack [*], Michael Schlegel [†], Marek Morzynski [‡]
and Gilead Tadmor [+]

[*] Institut Pprime, CNRS – Université de Poitiers – ENSMA, UPR 3346, Département Fluides, Thermique, Combustion, CEAT, 43, rue de l'Aérodrome, F-86036 Poitiers cedex, France

[†] Berlin Institute of Technology MB1, Department of Fluid Dynamics and Engineering Acoustics, Straße des 17. Juni 135, D-10623 Berlin, Germany

[‡] Technical University of Poznań, Institute of Combustion Engines and Transportation, ul. Piotrowo 3, PL 60-965 Poznań, Poland

[+] Northeastern University, Department of Electrical and Computer Engineering, 440 Dana Research Building, Boston, MA 02115, USA

Abstract A Galerkin method is presented for control-oriented reduced-order models (ROM). This method generalizes linear approaches elaborated by M. Morzyński et al. for the nonlinear Navier-Stokes equation. These ROM are used as plants for control design in the chapters by G. Tadmor et al., S. Siegel, and R. King in this volume. Focus is placed on empirical ROM which compress flow data in the proper orthogonal decomposition (POD). The chapter shall provide a complete description for construction of straight-forward ROM as well as the physical understanding and teste

1 Introduction

In the previous chapter by M. Morzyński et al., stability analysis was introduced as one foundation for control-oriented reduced-order models (ROM). These ROM constitute least-order descriptions optimized for linear flow dynamics. Here, the mathematical framework is extended to traditional Galerkin methods employing a larger class of expansion modes and resolving fully the nonlinear dynamics. The following chapters by G. Tadmor et al. and R. King in this volume will provide control studies based on the Galerkin method.

The current chapter is organized as follows: First (§2), the traditional Galerkin method is elaborated. This includes dynamic models based on the stability eigenmodes and the proper orthogonal decomposition (POD). In §3, a modal refinement of statistical fluid mechanics is outlined. This includes a novel closure for the first and second statistical moments based on

finite-time thermodynamics (Andresen, 1983). The resulting modal balance equations give important insights in the modal interactions and serve as design tool in model development. In §4, key enablers for control-oriented Galerkin models of turbulent flows are revisited. The conclusions (§5) summarize the previous chapters and outline challenges for future research.

2 Galerkin method as foundation

Focus of this section is a traditional *Galerkin method* for incompressible flow (Fletcher, 1984). This method shall approximately solve an initial boundary value problem which is formulated in §2.1. The postulates of the method are outlined in §2.2. The approximation ansatz is a finite *Galerkin expansion* in terms of global modes (§2.3). The derivation of the evolution equation for the mode amplitudes, the *Galerkin system*, is described in §2.4. In §2.5, we revisit this derivation for stability eigenmodes elaborated by M. Morzyński et al. in his chapter. A popular empirical realization is the proper orthogonal decomposition (POD), which minimizes a residual for a given data ensemble (§2.6). In general, this Galerkin method can approximate the flow evolution over a finite time horizon and may even reproduce the main characteristics of the long-term behavior.

2.1 Problem formulation

The incompressible, viscous flow is described in a Cartesian coordinate system $\boldsymbol{x} = (x, y, z)$ in the finite steady domain Ω. The x-, y- and z-axes are described by unit vectors $\boldsymbol{e}_x$, $\boldsymbol{e}_y$, $\boldsymbol{e}_z$, respectively. For the cylinder wake, the x-axis is aligned with the flow, the y-axis parallel to the shear and the z-axis parallel to cylinder axis. The velocity $\boldsymbol{u} = (u, v, w)$ has the components u, v and w in x-, y-and z-direction, respectively. The time is denoted by t and considered in the interval $[0, T]$. The pressure field is represented by p. The Cartesian components may also be indicated by indices, e.g. $\boldsymbol{x} = (x_1, x_2, x_3)$ or $\boldsymbol{u} = (u_1, u_2, u_3)$. An analogous convention applies to the unit vectors $\boldsymbol{e}_1$, $\boldsymbol{e}_2$, $\boldsymbol{e}_3$.

Kinematically, the flow is characterized by D, a characteristic length of the geometry, and U, a characteristic velocity. For the flow around the cylinder, D is chosen to be the diameter and U the oncoming velocity. The Newtonian fluid has constant density ρ and dynamic viscosity μ. In the following, we assume that all dependent and independent variables are non-dimensionalized with D, U, ρ and μ. The flow is characterized by the Reynolds number $Re = \rho U D/\mu$ or, equivalently, by its reciprocal denoted by $\nu := 1/Re$.

For the formulation of the initial boundary value problem (IBVP), we introduce ∂_x, ∂_y, ∂_z, and ∂_t for derivatives with respect to x, y, z and t. Alternatively, ∂_α indicates a derivate in the α-th Cartesian direction. Second derivatives are denoted similarly, e.g. ∂^2_{xx} for the second derivative with respect to x. The Nabla operator $\boldsymbol{\nabla} := (\partial_x, \partial_y, \partial_z)$ comprises first derivatives in a vector. The Laplace operator $\triangle := \partial^2_{xx} + \partial^2_{yy} + \partial^2_{zz}$ can act on a scalar or on a vector by acting on each Cartesian component.

We employ tensor algebra for products of scalars (0-th order tensors), vectors (1st order tensors) and matrices (representing 2nd-order tensors). The product between two tensors is by default an outer product, e.g. $\boldsymbol{\nabla u} = (\partial_\alpha u_\beta)$ represents the Jacobian of the velocity field. Similarly, $\boldsymbol{uu} := (u_\alpha u_\beta)$ denotes the dyadic product (a matrix). Inner products are denoted by $\cdot$ and contract the inner indices. Let $\boldsymbol{a}$ and $\boldsymbol{b}$ be two vectors, then $\boldsymbol{a} \cdot \boldsymbol{b} := \sum_{\alpha=1}^{3} a_\alpha b_\alpha$ represents the standard Euclidean product yielding a scalar. Let $\boldsymbol{A}$ be a matrix, then $\boldsymbol{A} \cdot \boldsymbol{b} := \sum_{\alpha=1}^{3} \boldsymbol{e}_\alpha \left(\sum_{\beta=1}^{3} A_{\alpha\beta} b_\beta \right)$. For later reference, we introduce the double contraction ': '. Let $\boldsymbol{A}$ and $\boldsymbol{B}$ two matrices, then $\boldsymbol{A} : \boldsymbol{B} := \sum_{\alpha=1}^{3} \sum_{\beta=1}^{3} A_{\alpha\beta} B_{\beta\alpha}$. Details can be inferred from any text book of tensor algebra.

It should be emphasized that tensor algebra and linear algebra have quite different notations. In tensor algebra the indices are tied to physical space and imply well-defined behavior for physical coordinate transformations. In linear algebra, vectors and matrices are just book-keeping quantities and the elements having no a priori meaning or transformation properties. Also the mathematics is different. Let $\boldsymbol{A}$ be a matrix and $\boldsymbol{b}$ a vector. Then $\boldsymbol{Ab}$ represents an outer product leading to a 3-rd order tensor in tensor algebra and inner product yielding a vector in matrix algebra. To cleanly separate both worlds, we keep round brackets for tensors and introduce square brackets for elements of linear algebra.

The evolution of the flow obeys mass and momentum balance, i.e. the equation of continuity and Navier-Stokes equation:

$$\boldsymbol{\nabla} \cdot \boldsymbol{u} = 0, \tag{1a}$$

$$\partial_t \boldsymbol{u} + \boldsymbol{\nabla} \cdot (\boldsymbol{u}\,\boldsymbol{u}) = -\boldsymbol{\nabla} p + \nu \triangle \boldsymbol{u} + \boldsymbol{g}\, b \tag{1b}$$

The flow is actuated with a simple volume force $\boldsymbol{g}(\boldsymbol{x})\, b(t)$ with a steady carrier field $\boldsymbol{g}$ and time-dependent amplitude b. An example is a Lorentz force of magnetohydrodynamics or a buoyancy term in the Boussinesq approximation.

A unique solution of (1) is expected when completed with an initial condition at time $t = 0$ and a boundary condition on the domain boundary $\partial\Omega$ in the integration time interval $[0, T]$. These conditions typically read

$$\boldsymbol{u}(\boldsymbol{x}, 0) = \boldsymbol{u}_{IC}(\boldsymbol{x}) \quad \forall \boldsymbol{x} \in \Omega, \tag{2}$$

$$\boldsymbol{u}(\boldsymbol{x}, t) = \boldsymbol{u}_{BC}(\boldsymbol{x}) \quad \forall \boldsymbol{x} \in \partial\Omega,\ t \in [0, T]. \tag{3}$$

We assume $\boldsymbol{u}_{IC} = \boldsymbol{u}_{BC}$ for $\boldsymbol{x} \in \partial\Omega$. The Dirichlet boundary condition (3) may be the no-slip condition on the wall or the free-stream condition at infinity. The following considerations can easily be applied also to periodic boundary conditions in nominally homogeneous directions or convective outflow conditions. The initial boundary value problem (1),(2),(3) defines flows around obstacles, like spheres, cylinders and airfoils, in uniform stream as well as most internal flows.

Typically, the pressure is considered as a Lagrange multiplier ensuring incompressibility (1a). The pressure can be computed from the velocity field by taking the divergence of (1b) and exploiting (1a). This yields the pressure-Poisson equation,

$$\triangle p = -(\boldsymbol{\nabla}\boldsymbol{u})^{\top} : \boldsymbol{\nabla}\boldsymbol{u}. \tag{4}$$

Here, the superscript $\top$ denotes a transpose (exchange of indices) in the velocity Jacobian. At the boundary, the multiplication of (1b) with the wall normal $\boldsymbol{n}$ yields a Robins boundary condition for p. This condition and (4) define p uniquely up to an arbitrary constant. The constant does not affect the velocity field. Hence, we can consider the Navier-Stokes residual

$$\boldsymbol{R}(\boldsymbol{u}) := \partial_t \boldsymbol{u} + \boldsymbol{\nabla} \cdot (\boldsymbol{u}\,\boldsymbol{u}) + \boldsymbol{\nabla} p - \nu \triangle \boldsymbol{u} - \boldsymbol{g}\, b \tag{5}$$

as a function of the velocity field only.

The above consideration apply to low-Mach number flows of Newtonian fluids in steady domains. The consideration does not include compressibility (e.g. transonic or supersonic flows), wall motion (e.g. aeroelastics) and combustion (or other multi-physics phenomena).

2.2 Traditional Galerkin method

The Galerkin method (Fletcher, 1984) approximates the solution of the IBVP (1), (2), (3) in the form

$$\boldsymbol{u}^{[0\ldots N]}(\boldsymbol{x}, t) = \boldsymbol{u}_0(\boldsymbol{x}) + \sum_{i=1}^{N} a_i(t)\, \boldsymbol{u}_i(\boldsymbol{x}) \tag{6a}$$

$$\frac{d}{dt}\boldsymbol{a} = \boldsymbol{f}^{[0\ldots N]}(\boldsymbol{a}, b)\,. \tag{6b}$$

Here, the velocity field is approximated by $\boldsymbol{u}^{[0\ldots N]}$, a finite expansion in terms of the base flow $\boldsymbol{u}_0$, N space-dependent modes $\boldsymbol{u}_i$ and corresponding time-dependent mode amplitudes a_i. The evolution equation is compressed in a system of ordinary differential equations for the mode amplitudes $\boldsymbol{a} := [a_1, \ldots, a_N]^\top$ via the propagator $\boldsymbol{f}^{[0\ldots N]} = \left[f_1^{[0\ldots N]}, \ldots, f_N^{[0\ldots N]}\right]^\top$. The control command b is included in (6b) to match (1b). The bulky superscript $[0\ldots N]$ shall remind which index set of modes is employed in the approximation and may be omitted without warning.

Almost any computational solution method of the Navier-Stokes equation can be framed in the form (6). The particularity of the *traditional* Galerkin method is aiming at a low dimension N as first priority. This method is deeply rooted in functional analysis and has following properties:

GM1: The incompressibility (1a) is exactly fulfilled for all choices of mode amplitudes.

GM2: The boundary condition (3) is exactly fulfilled for all choices of mode amplitudes.

GM3: The modes are a subset of a complete orthonormal system (ONS) $\{\boldsymbol{u}_i\}_{i=0}^{\infty}$ of the Hilbert space of square integrable vector fields $L^2(\Omega)$, or an Hilbert subspace $H(\Omega) \subset L^2(\Omega)$ guaranteeing a problem-specific, sufficiently high regularity of the considered functions. The Hilbert space $L^2(\Omega)$ is equipped with an inner product between two vector fields $\boldsymbol{v}$ and $\boldsymbol{w}$

$$(\boldsymbol{v}, \boldsymbol{w})_\Omega := \int_\Omega d\boldsymbol{x}\, \boldsymbol{v} \cdot \boldsymbol{w} \tag{7}$$

and the associated norm

$$\|\boldsymbol{v}\|_\Omega := \sqrt{(\boldsymbol{v}, \boldsymbol{v})_\Omega}. \tag{8}$$

Orthonormality of the modes reads

$$\forall i, j \in \{1, \ldots, N\} \quad : \quad (\boldsymbol{u}_i, \boldsymbol{u}_j)_\Omega = \delta_{ij}. \tag{9}$$

The completeness of the ONS implies that an arbitrary accuracy of (6a) is achievable by increasing the mode number N.

GM4: The ansatz should be compatible with the weak solution of the Navier-Stokes equation, i.e.

$$\forall \boldsymbol{v} \in H(\Omega) \quad : \quad (\boldsymbol{v}, \boldsymbol{R}(\boldsymbol{u}))_\Omega = 0\,, \tag{10}$$

where $\boldsymbol{R}$ represents the Navier-Stokes operator based on generalized derivatives.

The numbering of the postulate reflects its relative importance in the traditional Galerkin method. Property *GM3* implies that the resolution accuracy is controlled by the number of global modes, defined on the whole domain Ω. No existence of grid is implied or necessary in this analytical framework. Property *GM3* discriminates the traditional Galerkin method from grid-based discretizations of the Navier-Stokes equation, like finite-difference, finite-volume or finite-element schemes. Here, the local modes are tied to the grid and an increasing grid resolution requires a new set of modes. A rigorous mathematical theory detailing *GM4* and other aspects is outside the scope of this book. Instead, we refer to the classics by Ladyzhenskaya (1963).

2.3 Galerkin expansion

In this section, properties of the Galerkin expansion (6a) are derived. The first property *GM1* of the previous section implies

$$\boldsymbol{\nabla} \cdot \boldsymbol{u}_i = 0, \quad i = 0, 1, \ldots, N. \tag{11}$$

This condition liberates us from re-considering the mass balance (1a) in future considerations.

The second property *GM2* yields

$$\forall \boldsymbol{x} \in \partial\Omega \quad : \quad \boldsymbol{u}_0(\boldsymbol{x}) = \boldsymbol{u}_{BC}(\boldsymbol{x}) \quad \text{and} \quad \boldsymbol{u}_i(\boldsymbol{x}) = 0, \quad i = 1, \ldots, N. \tag{12}$$

Now, the boundary conditions are incorporated.

The third property *GM3* allows to determine the mode amplitudes for a given velocity field $\boldsymbol{u}$ by minimizing the residual $\left\|\boldsymbol{u} - \boldsymbol{u}^{[0\ldots N]}\right\|_\Omega$:

$$a_i = (\boldsymbol{u} - \boldsymbol{u}_0, \boldsymbol{u}_i)_\Omega \,. \tag{13}$$

It should be noted that the mode amplitude a_i is not distorted by the orthogonal residual $\sum_{i=N+1}^{\infty} a_i \boldsymbol{u}_i$ of the Galerkin expansion, i.e. is independent of N.

The energy content of the fluctuation $\boldsymbol{u}' := \boldsymbol{u} - \boldsymbol{u}_0 = \sum_{i=1}^{\infty} a_i \boldsymbol{u}_i$ is quantified by the instantaneous fluctuation energy

$$K(t) = \frac{1}{2} \, \|\boldsymbol{u}'\|_\Omega^2 \,. \tag{14}$$

In statistical fluid mechanics, K is also termed turbulent kinetic energy (*TKE*). The orthogonality of the modes allows to partition K into modal

energies $K_i(t)$, the energy content of each modal subspace contribution $\boldsymbol{u}^{[i]} = a_i\, \boldsymbol{u}_i$:

$$K(t) = \sum_{i=1}^{\infty} K_i(t), \quad \text{where} \quad K_i(t) := \frac{1}{2} \left\| \boldsymbol{u}^{[i]} \right\|_{\Omega}^2 = \frac{1}{2}\, a_i^2. \tag{15}$$

For later reference, we note that (14) and (15) refer to the instantaneous values of the energies. By default, K and K_i represent averaged values if the argument '(t)' is omitted.

2.4 Galerkin system

Finally, we derive the evolution equation of the mode amplitudes. The finite Galerkin expansion (6a) cannot be expected to yield an exact solution of (10) under general conditions. However, (10) can be exactly satisfied for all test functions from the same subspace as the Galerkin expansion. Without loss of generality, we choose the N expansion modes as test functions:

$$\left(\boldsymbol{u_i}, \boldsymbol{R}\left(\boldsymbol{u}^{[0\ldots N]} \right) \right)_{\Omega}, \quad i = 1, \ldots, N. \tag{16}$$

This step is called *Galerkin projection*, we project the Navier-Stokes equation on the subspace of the Galerkin expansion.

To simplify the Galerkin projection, we re-write (6a) as

$$\boldsymbol{u}^{[0\ldots N]} = \sum_{i=0}^{N} a_i \boldsymbol{u}_i, \tag{17}$$

where $a_0 \equiv 1$. Moreover we introduce $(F)_{\Omega} := \int_{\Omega} d\boldsymbol{x}\, F$ as notation for the volume integral of F over the domain. $[F]_{\partial\Omega} := \oint_{\partial\Omega} d\boldsymbol{A} \cdot F$ represents the surface integral of F over the boundary of the domain. F is typically a scalar, like pressure, but could also be a vector or higher-order tensor.

The projection of the local acceleration term reads

$$\left(\boldsymbol{u}_i, \partial_t \left[\sum_{j=0}^{N} a_j \boldsymbol{u}_j \right] \right)_{\Omega} = \sum_{j=1}^{N} \dot{a}_j \left(\boldsymbol{u}_i, \boldsymbol{u}_j \right)_{\Omega} = \dot{a}_i, \tag{18}$$

exploiting the steadiness of a_0 and the orthonormality of the modes (9). The Galerkin projection of the viscous term yields

$$\left(\boldsymbol{u}_i, \nu \triangle \left[\sum_{j=0}^{N} a_j \boldsymbol{u}_j \right] \right)_{\Omega} = \nu \sum_{j=0}^{N} l_{ij}^{\nu}\, a_j, \tag{19a}$$

$$l_{ij}^{\nu} = \left(\boldsymbol{u}_i, \triangle \boldsymbol{u}_j \right)_{\Omega} = \left[\boldsymbol{u}_i \cdot \boldsymbol{\nabla} \boldsymbol{u}_j \right]_{\partial\Omega} - \left(\boldsymbol{\nabla} \boldsymbol{u}_i \colon \boldsymbol{\nabla} \boldsymbol{u}_j \right)_{\Omega} \tag{19b}$$

The transformation of l^ν_{ij} to a term with first derivatives has been performed employing Green's identity. Numerically, the transformed term generally leads to more accurate values of l^ν_{ij} and is hence preferred. For Dirichlet boundary conditions, the surface integral vanishes, since $\boldsymbol{u}_i \equiv 0$ on the domain boundary. In this case, l^ν_{ij} represents a negative semi-definite matrix. Note that (19) is linear ('pseudo-linear') in $[a_0, \ldots, a_N]^\top$ but contains a constant term at $j = 0$ with respect to the non-trivial mode amplitudes $[a_1, \ldots, a_N]^\top$.

The Galerkin projection of the convective term leads to a pseudo-quadratic form

$$\left(\boldsymbol{u}_i, -\boldsymbol{\nabla}\cdot\left(\left[\sum_{j=0}^{N} a_j\boldsymbol{u}_j\right]\left[\sum_{k=0}^{N} a_k\boldsymbol{u}_k\right]\right)\right)_\Omega = \sum_{j=0}^{N}\sum_{k=0}^{N} q^c_{ijk}a_j a_k \tag{20a}$$

$$q^c_{ijk} = -\left(\boldsymbol{u}_i, \boldsymbol{\nabla}\cdot(\boldsymbol{u}_j\boldsymbol{u}_k)\right)_\Omega . \tag{20b}$$

For the Galerkin projection of the pressure term, we first construct a solution of the pressure-Poisson equation with respect to p. Let p_{jk}, termed 'partial pressures' in the sequel, satisfy

$$\triangle p_{jk} = -\left(\boldsymbol{\nabla}\boldsymbol{u}_j\right)^\top : \boldsymbol{\nabla}\boldsymbol{u}_k. \tag{21}$$

Then, the pseudo-quadratic Galerkin ansatz of the pressure

$$p^{[0\ldots N]}(\boldsymbol{x}, t) = \sum_{j=0}^{N}\sum_{k=0}^{N} p_{jk}(\boldsymbol{x})\, a_j(t)\, a_k(t) \tag{22}$$

satisfies the pressure-Poisson equation (4) neglecting the residual of the Galerkin expansion. Employing (22), the Galerkin projection of the pressure term becomes

$$\left(\boldsymbol{u}_i, -\boldsymbol{\nabla}p^{[0\ldots N]}\right)_\Omega = \sum_{j=0}^{N}\sum_{k=0}^{N} q^p_{ijk}a_j\, a_k \tag{23a}$$

$$q^p_{ijk} = -\left(\boldsymbol{u}_i, \boldsymbol{\nabla}\cdot p_{jk}\right)_\Omega = -\left[\boldsymbol{u}_i p_{jk}\right]_{\partial\Omega} . \tag{23b}$$

In the second transformation of q^p_{ijk}, the incompressibility of the modes and Gauss integral formula is exploited. Note that this surface integral vanishes for Dirichlet boundary conditions (3), implying (12) for the modes. In this case, the pressure-term representation vanishes identically in the Galerkin projection. This behavior is consistent with the interpretation of pressure as a Lagrange multiplier for incompressibility. The pressure has no role to

play on the solenoidal affine space spanned by the Galerkin expansion (6a). The same statement applies also to periodic boundary conditions, as proven in Holmes et al. (1998).

In case of open flows with convective boundary conditions, the modes do not vanish identically on the boundary and the pressure term may play an important role (Noack et al., 2005; Noack, 2006). We refer to these original papers for the details on the incorporation of the boundary conditions in (4), (21).

In practice, the computation of partial pressures p_{jk} is numerically delicate and expensive. Past studies (Noack et al., 2005; Noack, 2006) indicate that the effect of the pressure term is well accounted by a linear term. In fact, most authors employ a calibrated linear term to account for the pressure term — starting with Galletti et al. (2004). We decompose the pressure in a constant part $p^c = p_{00}$, a linear (so called 'fast') term $p^l = \sum_{j=1}^{N} (p_{j0} + p_{0j})\, a_j$, and a quadratic (so called 'slow') contribution $p^q = \sum_{j,k=1}^{N} p_{jk}\, a_j\, a_k$, respectively:

$$p = p^c + p^l + p^q. \tag{24}$$

The constant component may drive internal flows, like the pressure gradient in pipe flow. For open flows, the Galerkin representation of this part tends to be negligible. The quadratic component tends to be small compared to linear pendant (Noack, 2006), justifying a posteriori the calibrated linear term.

As a historical note, the pioneering work of Aubry et al. (1988) emphasized already the potentially important role of the pressure term, but did not propose a physics-based model. Rempfer and Fasel (1994) bypassed the modeling problem by projection on the pressure-free vorticity equation. This projection lumps the effect of the convection- and the pressure-term in a single term

$$q_{ijk} = q^c_{ijk} + q^p_{ijk} \quad j,k = 0,\ldots,N. \tag{25}$$

Finally, the Galerkin projection of the volume force term reads

$$(\boldsymbol{u}_i, \boldsymbol{g}\, b)_\Omega = g_i\, b, \quad \text{where} \quad g_i = (\boldsymbol{u}_i, \boldsymbol{g})_\Omega\,. \tag{26}$$

Summarizing, the projection (16) yields following Galerkin system:

$$\underbrace{\dot{a}_i}_{\substack{\text{local}\\ \text{acceleration}}} = \underbrace{\nu \sum_{j=0}^{N} l_{ij}^{\nu}\, a_j}_{\substack{\text{viscous}\\ \text{term}}} + \underbrace{\sum_{j,k=0}^{N} q_{ijk}^{c}\, a_j\, a_k}_{\substack{\text{convective}\\ \text{term}}} + \underbrace{\sum_{j,k=0}^{N} q_{ijk}^{p}\, a_j\, a_k}_{\substack{\text{pressure}\\ \text{gradient}}} + \underbrace{g_i b}_{\substack{\text{volume}\\ \text{force}}} \quad . \tag{27}$$

The form elegantly allows to trace back each term from the corresponding Navier-Stokes pendant. However, dynamical system analyses are complicated by the inclusion of $a_0 \equiv 1$. Examples include finding the fixed point and performing a stability analysis. Hence, we re-write (27) in the form

$$\dot{a}_i = c_i + \sum_{j=1}^{N} l_{ij}\, a_j + \sum_{j,k=1}^{N} q_{ijk}\, a_j\, a_k + g_i b, \tag{28}$$

where $c_i = \nu\, l_{i0} + q_{i00}^{c} + q_{i00}^{p}$, $l_{ij} = \nu\, l_{ij}^{\nu} + q_{ij0}^{c} + q_{i0j}^{c} + q_{ij0}^{p} + q_{i0j}^{p}$, and q_{ijk} is defined by (25). Note that the constant term c_i would vanish if $\boldsymbol{u}_0$ is chosen to be a steady Navier-Stokes solution.

2.5 Non-orthogonal modes

The eigenmodes of stability analysis are generally not orthogonal to each other. In this case, we introduce a mass matrix $\boldsymbol{M} = (m_{ij})$, where $m_{ij} := (\boldsymbol{u}_i, \boldsymbol{u}_j)_\Omega$ and the Galerkin projection leads to

$$\sum_{j=1}^{N} m_{ij}\, \dot{a}_j = \nu \sum_{j=0}^{N} l_{ij}^{\nu}\, a_j + \sum_{j,k=0}^{N} q_{ijk}^{c}\, a_j\, a_k + \sum_{j,k=0}^{N} q_{ijk}^{p}\, a_j\, a_k + g_i b. \tag{29}$$

The local acceleration term on the left-hand side is generalized, but all terms on the right-hand side remain unaltered. This equation can be solved for $\dot{a}_i$ by multiplication with the inverse mass matrix. An alternative yet equivalent trick is the use of adjoint modes $\boldsymbol{v}_i$ as test functions in the Galerkin projection (Haken, 1983):

$$\left(\boldsymbol{v}_i, \boldsymbol{R}\left(\boldsymbol{u}^{[0\ldots N]}\right)\right)_\Omega, \quad i = 1, \ldots, N. \tag{30}$$

The adjoint and original modes satisfy the orthogonality relationship $(\boldsymbol{u}_i, \boldsymbol{v}_j)_\Omega = \delta_{ij}$. Thus, Galerkin projection leads to (27), again.

2.6 POD models

The main art of Galerkin modeling is constructing a good low-dimensional 'modal piano.' The modes should span a subspace in which the attractor and nearby transients are well resolved.

Common choices of the basic mode $\boldsymbol{u}_0$ are the steady solution or the mean flow. Both fulfill the incompressibility (1a) and the boundary conditions (3). In principle, any velocity field satisfying these conditions serve the purpose. In practice, the choice of the basic mode is not overly critical if the expansion modes can compensate for deviations of the base flow.

In contrast, the performance of the Galerkin method depends quite sensitively on the choice of the expansion modes. In principle, the Hilbert space of square-integrable solenoidal velocity fields guarantees the existence of a complete orthonormal system. This property is exploited by *mathematical* approaches which are successfully applied to geometrically simple internal flows (Lorenz, 1963; Busse, 1991) but also to open flows (Noack and Eckelmann, 1994a,b). The method poses severe analytical and numerical challenges for general 3D geometries. These challenges have excluded an application for most engineering tasks. Moreover, the advantage of the mathematical modes, guaranteed completeness independently of the evolution equation to be approximated, is at the same time a weakness in terms of the required low dimensions.

A more problem-tailored *physical* method is a Galerkin model based on stability eigenmodes of a linearized Navier-Stokes related equation, like Stokes equation (Joseph, 1976), a modified Stokes equation (Batcho, 1994), or the constitutive equation of stability analysis (see the chapter of M. Morzyński et al.). This approach can be expected to lead to lower-order expansions since it includes properties of the evolution equation. However, the property of completeness of the stability eigenmodes has only been proven for very few highly symmetrical configurations (Joseph, 1976; Grosch and Salwen, 1978; Salwen and Grosch, 1981) and may be questionable for open flows. Physical Galerkin models have been constructed for internal flows (Rummler, 2000), for wakes (Afanasiev, 2003) and for the flow over a cavity (Åkervik et al., 2007).

A third *empirical* ansatz employs experimental or simulation flow data from the target configuration. Often, the most energetic directions are extracted from snapshots $\boldsymbol{u}^m$, $m = 1, \ldots, M$ in the observation domain Ω. A canonical approach, is called principle axis, Karhunen-Lòeve or *proper orthogonal decomposition* (POD). Let $\langle \quad \rangle_M$ denote the average over these snapshots. Then, POD optimizes the averaged residual with respect to the L_2-norm. In other words, any other N-dimensional expansion $\boldsymbol{w}^{[0\ldots N]} =$

$\sum_{i=0}^{N} c_i \boldsymbol{w}_i$ of which the modes $\{\boldsymbol{w}_i\}_{i=0}^{N}$ satisfy incompressibility (11), the boundary conditions (12) and orthonormality (9) cannot have a smaller residual:

$$\langle \|\boldsymbol{u}^m - \sum_{i=0}^{N} a_i^m \boldsymbol{u}_i\|_\Omega^2 \rangle_M \leq \langle \|\boldsymbol{u}^m - \sum_{i=0}^{N} c_i^m \boldsymbol{w}_i\|_\Omega^2 \rangle_M . \tag{31}$$

Here, the superscript m of the snapshot is transferred to the mode amplitudes. Apart from there usefulness for data compression, the POD modes have no inherent physical meaning. For the soft onset of oscillatory fluctuations, mean-field theory derives that the first 2 POD modes span the real and imaginary part of the unstable complex stability eigenmode. Similarity between selected POD modes and stability eigenmodes has been observed for several configurations. In general, POD does not extract pure frequency modes, like stability eigenmodes. Dynamic mode decomposition (DMD) is another data-driven flow decomposition designed to match stability eigenmodes under suitable conditions (Rowley et al., 2009; Schmid, 2010). DMD trades the optimal resolution efficiency of POD against distillation of pure eigenfrequencies in short-time sampled data.

The construction of POD modes can be inferred from many excellent sources (Holmes et al., 1998). The modes are best conceptualized as principle axes of a Gaussian distribution fitted to the snapshots representing the first and second moments (Cordier and Bergmann, 2003). Typically, the number of POD modes is chosen much smaller than the number of snapshots, $N \ll M$. The maximum of number of modes reads $N = M - 1$, since M points span a $M - 1$-dimensional manifold.

Snapshot-based POD consists of 5 steps (Sirovich, 1987):

1. Compute the mean flow,

$$\boldsymbol{u}_0 := \frac{1}{M} \sum_{m=1}^{M} \boldsymbol{u}^m . \tag{32}$$

2. Compute the correlation matrix $\boldsymbol{C} = (C^{mn})$ of the fluctuations,

$$C^{mn} := \frac{1}{M} \left(\boldsymbol{u}^m - \boldsymbol{u}_0, \boldsymbol{u}^n - \boldsymbol{u}_0\right)_\Omega . \tag{33}$$

   Note that $\boldsymbol{C}$ is a symmetric positive semi-definite gramian matrix.

3. Perform the spectral analysis of this matrix, i.e. find the first N eigenvectors $\boldsymbol{e}_i = \left[e_1^i, \ldots, e_M^i\right]^\top$ and sorted eigenvalues $\lambda_1 \geq \lambda_2 \geq \ldots \geq \lambda_N \geq 0$,

$$\boldsymbol{C}\boldsymbol{e}_i = \lambda_i \boldsymbol{e}_i, \quad i = 1, \ldots, N. \tag{34}$$

Without loss of generality, the eigenvectors are assumed to be orthonormalized, $\boldsymbol{e}_i \cdot \boldsymbol{e}_j = \delta_{ij}$, thanks to the symmetry of $\boldsymbol{C}$.

4. Compute each POD mode as linear combination of the snapshot fluctuations,

$$\boldsymbol{u}_i := \frac{1}{\sqrt{M\,\lambda_i}} \sum_{m=1}^{M} e_m^i \, (\boldsymbol{u}^m - \boldsymbol{u}_0)\,, \quad i = 1, \ldots, N. \tag{35}$$

The POD modes satisfy the orthonormality condition (9).

5. Compute the mode amplitudes,

$$a_i^m := \sqrt{\lambda_i \, M}\, e_m^i, \quad i = 1, \ldots, N. \tag{36}$$

These amplitudes vanish on average and are uncorrelated (orthogonal in time),

$$\langle a_i \rangle_M = 0, \quad \langle a_i a_j \rangle_M = \lambda_i \, \delta_{ij}, \quad i, j \in \{1, \ldots, N\}. \tag{37}$$

POD defines a second-order statistics providing the mean flow $\boldsymbol{u}_0$ and the two-point autocorrelation function

$$\overline{\boldsymbol{u}'(\boldsymbol{x}, t)\, \boldsymbol{u}'(\boldsymbol{y}, t)} = \sum_{i=1}^{N} \lambda_i \, \boldsymbol{u}_i(\boldsymbol{x})\, \boldsymbol{u}_i(\boldsymbol{y}). \tag{38}$$

Hence, a minimum requirement to the snapshot ensemble is the accuracy of the derived mean flow and the second moments. Accuracy of the statistics for a given number of snapshots is increased by uncorrelated snapshots as required in the original paper on the snapshot POD method (Sirovich, 1987).

POD is optimal for the given data set in the sense of (31), but is generically not complete (violates *GM3*). Applicability for other Reynolds numbers, for transients and for actuation is very restricted (Deane et al., 1991). Numerous suggestions have been made to improve or augment POD for several operating conditions. We refer the interested reader to the literature (Ma and Karniadakis, 2002; Noack et al., 2003; Jørgensen et al., 2003; Siegel et al., 2008).

The Galerkin projection can be effected on any orthonormal(ized) set of modes. It has become increasingly common to add calibrated corrections to the constant and linear terms (Galletti et al., 2004; Tadmor and Noack, 2004). These corrections shall account for the pressure term, the neglected modes, mode deformations or other diseases of the Galerkin method. The calibration of the whole Galerkin system with constant, linear, and quadratic terms is generally badly conditioned and should invoke a penalization procedure for the quadratic terms (Cordier et al., 2010).

POD Galerkin models have been constructed for practically all flow configurations. Examples are Couette flow (Moehlis et al., 2002), transitional (Rempfer and Fasel, 1994) and turbulent boundary layers (Aubry et al., 1988; Podvin, 2009), wakes (Deane et al., 1991; Noack et al., 2003), mixing layers (Ukeiley et al., 2001; Noack et al., 2005; Wei and Rowley, 2009), jets (Schlegel et al., 2009). The vast amount of published successful POD models should not mislead the reader to assume that they can be easily constructed with the standard approach, or that they are robust. Most models are fragile and critically dependent on additional enablers, such as discussed in §4.

3 Statistical fluid mechanics as design tool

POD can be considered as a refinement of the Reynolds decomposition of velocity field. The fluctuation is decomposed in modal compartments,

$$\boldsymbol{u} = \boldsymbol{u}_0 + \boldsymbol{u}', \quad \boldsymbol{u}' = \sum_{i=1}^{\infty} \boldsymbol{u}^{[i]}, \quad \boldsymbol{u}^{[i]} = a_i \boldsymbol{u}_i. \tag{39}$$

In this section, we refine some well-known equations of statistical fluid mechanics for the fluctuation (Monin and Yaglom, 1971, 1975) into the modal pendants. First (§3.1), the principles of global and modal balance equations are revisited. The modal pendants of the Reynolds and TKE equation are presented in §3.2. Finally, a novel closure for the first and second moments of Galerkin systems is outlined (§3.3). The balance equations of this section can be employed as powerful analysis and design tool. Examples are understanding the modal interactions, checking the accuracy of the numerical data, evaluating the (reduced) Galerkin models, deriving free calibration parameters, and determining the analytical form of the subgrid turbulence models.

3.1 Principles of balance equations

Statistical fluid mechanics is based on a Reynolds average, denoted by an overbar $\overline{\ }$ or $\langle\ \ \rangle$. This average may be the infinite time mean, an ensemble average, a spatial average over one or more homogeneous directions, or any other filter satisfying the Reynolds properties (Monin and Yaglom, 1971). A large class of global balance equations for the domain Ω can derived from the average of (10)

$$\overline{(\boldsymbol{v}, \boldsymbol{R}(\boldsymbol{u}))_\Omega} = 0. \tag{40}$$

The weak form of the Reynolds equation is obtained by substituting the Reynolds decomposition in (40), and allowing any test function $\boldsymbol{v}$. Choosing

$\boldsymbol{v} = \boldsymbol{u}$, $\boldsymbol{u}_0$, or $\boldsymbol{u}'$ leads to global balance equation for the total kinetic energy, the mean flow or the TKE, respectively. The drag or lift formulae are derived by setting $\boldsymbol{v} = \boldsymbol{e}_x$ or $\boldsymbol{v} = \boldsymbol{e}_y$, respectively. As a slight variation, the Reynolds stress balance equations are inferred from the symmetric matrix valued equation:

$$\overline{(\boldsymbol{u}'\,\boldsymbol{R}(\boldsymbol{u}) + \boldsymbol{R}(\boldsymbol{u})\,\boldsymbol{u}')_\Omega} = 0\,, \tag{41}$$

representing the special case $\boldsymbol{v} = \boldsymbol{u}'$ of a larger class of balance equations given by

$$\overline{(\boldsymbol{v}\,\boldsymbol{R}(\boldsymbol{u}) + \boldsymbol{R}(\boldsymbol{u})\,\boldsymbol{v})_\Omega} = 0\,. \tag{42}$$

Modal pendants of the above mentioned global equations are obtained by substituting the POD (39) as argument in the Navier-Stokes residual and, if necessary, by replacements of the test function. The i-th modal Reynolds equation is obtained by setting $\boldsymbol{v} = \boldsymbol{u}_i$ in (40).

The i-th modal energy balance equation employs $\boldsymbol{v} = \boldsymbol{u}^{[i]}$ instead of $\boldsymbol{v} = \boldsymbol{u}'$ for the TKE equation. Note that the linearity of (40) in $\boldsymbol{v}$ allows to derive the original TKE from the modal compartments.

Similarly, the modal Reynolds stress balance equation is based on the similar trick: insert $\boldsymbol{v} = \boldsymbol{u}^{[i]}$ in (42). The global pendant is obtained by the sum of the original equation.

The effect of the modes on the energy of the mean flow, on the drag or on the lift can be assessed when the Reynolds decomposition is replaced by the POD in the original equation. Tab. 1 summarizes the discussion.

3.2 Modal balance equations

Detailing the discussion of the last section, we derive the modal Reynolds and TKE equation for POD modes. This derivation can be based on the Navier-Stokes equation or the Galerkin system (27), since there is a one-to-one correspondence between Navier-Stokes and Galerkin-system terms (see Tab. 2). We pursue the easier task based on deriving the balance equation from the dynamical system. Moreover, we assume accuracy of the finite Galerkin expansion with N modes and shall, at the moment, not pause to discuss the effect of the residual.

The Reynolds decomposition of the POD mode amplitudes reads

$$a_0 \equiv 1, \quad a_0' \equiv 0 \tag{43a}$$

$$a_i = a_i', \quad \overline{a_i} = 0 \quad i = 1, \ldots, N. \tag{43b}$$

The modal Reynolds equation is obtained by Reynolds-averaging the Galerkin system and exploiting (37). We chose the dynamical systems (28) for rea-

Table 1. Constitutive equations for selected global and modal balances.

quantity	global balance equation	modal balance equation
argument of $\boldsymbol{R}(\boldsymbol{u})$	$\boldsymbol{u} = \boldsymbol{u}_0 + \boldsymbol{u}'$	$\boldsymbol{u} = \sum_{j=0}^{\infty} \boldsymbol{u}^{[j]}$
Reynolds equation	(40) for all test functions $\boldsymbol{v}$	(40) for $\boldsymbol{v} = \boldsymbol{u}_i$
kinetic energy	(40) for $\boldsymbol{v} = \boldsymbol{u}_0 + \boldsymbol{u}'$	(40) for $\boldsymbol{v} = \sum_{j=0}^{\infty} \boldsymbol{u}^{[j]}$
mean flow kinetic energy	(40) for $\boldsymbol{v} = \boldsymbol{u}_0$	(40) for $\boldsymbol{v} = \boldsymbol{u}_0$
TKE / modal energy	(40) for $\boldsymbol{v} = \boldsymbol{u}'$	(40) for $\boldsymbol{v} = \boldsymbol{u}^{[i]}$
Reynolds stress	(42) for $\boldsymbol{v} = \boldsymbol{u}'$	(42) for $\boldsymbol{v} = \boldsymbol{u}^{[i]}$
drag	(40) for $\boldsymbol{v} = \boldsymbol{e}_x$	(40) for $\boldsymbol{v} = \boldsymbol{e}_x$
lift	(40) for $\boldsymbol{v} = \boldsymbol{e}_y$	(40) for $\boldsymbol{v} = \boldsymbol{e}_y$

sons of brevity:

$$0 = c_i + \sum_{j=1}^{N} 2 q_{ijj}\, K_j. \tag{44}$$

Here, c_i comprises the $\boldsymbol{u}_i$-projected Navier-Stokes residual of $\boldsymbol{u}_0$ and right term resolves the effect of the Reynolds stress and of the quadratic pressure term. There is only one energy distribution $K_i = \lambda_i/2$ consistent with the mean flow (N equations for N energy values). The linear term is averaged out and hence immaterial for POD modes.

The modal TKE equation is derived from the dynamical system by multiplying (28) with $a_i' = a_i$ and averaging:

$$\begin{aligned} \frac{d}{dt} K_i &= Q_i + T_i, \\ Q_i &:= 2\, l_{ii}\, K_i, \\ T_i &:= \sum_{j,k=1}^{N} T_{ijk}, \quad T_{ijk} := q_{ijk}\, \overline{a_i a_j a_k}. \end{aligned} \tag{45}$$

Table 2. Derivation diagram of the Galerkin system. In each column, all Navier-Stokes terms are listed. From top to bottom, the local acceleration, convective viscous and pressure gradient term are shown. From left to right, the Navier-Stokes equation is processed from the original form, to a form employing the Reynolds decomposition, and to a Galerkin projected form. Note that the Galerkin system on the right-most column can be aggregated form (27). with $a_0 \equiv 1$.

NSE	NSE with $\boldsymbol{u} = \boldsymbol{u}_0 + \boldsymbol{u}'$	Galerkin-projection	Galerkin-system
$\partial_t \boldsymbol{u} =$	$\partial_t \boldsymbol{u}' =$	$(\boldsymbol{u}_i, \partial_t \boldsymbol{u}')_\Omega =$	$\frac{d}{dt} a_i =$
$-\boldsymbol{\nabla} \cdot [\boldsymbol{u}\, \boldsymbol{u}]$	$-\boldsymbol{\nabla} \cdot [\boldsymbol{u}_0\, \boldsymbol{u}_0]$	$-(\boldsymbol{u}_i, \boldsymbol{\nabla} \cdot [\boldsymbol{u}_0\, \boldsymbol{u}_0])_\Omega$	q^c_{i00}
	$-\boldsymbol{\nabla} \cdot [\boldsymbol{u}'\, \boldsymbol{u}_0]$	$-(\boldsymbol{u}_i, \boldsymbol{\nabla} \cdot [\boldsymbol{u}'\, \boldsymbol{u}_0])_\Omega$	$+\sum_{j=1}^{N} q^c_{ij0} a_j$
	$-\boldsymbol{\nabla} \cdot [\boldsymbol{u}_0\, \boldsymbol{u}']$	$-(\boldsymbol{u}_i, \boldsymbol{\nabla} \cdot [\boldsymbol{u}_0\, \boldsymbol{u}'])_\Omega$	$+\sum_{j=1}^{N} q^c_{i0j} a_j$
	$-\boldsymbol{\nabla} \cdot [\boldsymbol{u}'\, \boldsymbol{u}']$	$-(\boldsymbol{u}_i, \boldsymbol{\nabla} \cdot [\boldsymbol{u}'\, \boldsymbol{u}'])_\Omega$	$+\sum_{j,k=1}^{N} q^c_{ijk} a_j a_k$
$+\nu \triangle \boldsymbol{u}$	$+\nu \triangle \boldsymbol{u}_0$	$+\nu\,(\boldsymbol{u}_i, \triangle \boldsymbol{u}_0)_\Omega$	$+\nu l_{i0}$
	$+\nu \triangle \boldsymbol{u}'$	$+\nu\,(\boldsymbol{u}_i, \triangle \boldsymbol{u}')_\Omega$	$+\nu \sum_{j=1}^{N} l^\nu_{ij} a_j$
$-\boldsymbol{\nabla} p$	$-\boldsymbol{\nabla} p_0$	$-(\boldsymbol{u}_i, \boldsymbol{\nabla} p_0)_\Omega$	$+q^p_{i00}$
	$-\boldsymbol{\nabla} p'$	$-(\boldsymbol{u}_i, \boldsymbol{\nabla} p')_\Omega$	$+\sum_{\substack{j,k=0 \\ \max\{j,k\}>0}}^{N} q^p_{ijk} a_j a_k$

The time-derivative of K_i does not generally vanish for finite POD snapshot ensembles. Q_i lumps the effect of all Navier-Stokes terms which are linear in $\boldsymbol{u}'$. A look on Tab. 2 and the pressure model will reveal that these terms contain either $\boldsymbol{u}_0$ or ν, i.e. describe interactions with the mean flow or with the molecular chaos. Hence, Q_i lumps the effect of *external* interactions with respect to the mode ensemble. In contrast, T_i aggregates the energy flow of *internal* triadic interactions T_{ijk} from the convection term and the

quadratic pressure term $p^{(2)}$. Hence, T_i is not effected by mean flow or viscosity.

A refined physical resolution of the modal TKE equation is obtained by repeating the operations for the Galerkin system (27). We shall refer to the Navier-Stokes equation. Tab. 3 elucidates the origin of the TKE terms, namely the production P, the convection C, the transfer T, the dissipation D and the pressure power F. Tab. 4 contains the modal pendant. Neglecting pressure terms, the external energy flow comprises production, convection and dissipation $Q_i = P_i + C_i + D_i$ while the transfer term T_i remains unaltered. In (45), the linear pressure term p^l of (24) contributes to Q_i and the quadratic term p^q to T_i.

Table 3. Derivation scheme of the global TKE equation.

NSE with $\boldsymbol{u} = \boldsymbol{u}_0 + \boldsymbol{u}'$	Galerkin projection on $\boldsymbol{u}'$	global energy flow balance (averaged)	do. (short form)
$\partial_t \boldsymbol{u}' =$	$(\boldsymbol{u}', \partial_t \boldsymbol{u}')_\Omega =$	$dK/dt =$	$dK/dt =$
$-\boldsymbol{\nabla} \cdot [\boldsymbol{u}_0\, \boldsymbol{u}_0]$	$-(\boldsymbol{u}', \boldsymbol{\nabla} \cdot [\boldsymbol{u}_0\, \boldsymbol{u}_0])_\Omega$		
$-\boldsymbol{\nabla} \cdot [\boldsymbol{u}'\, \boldsymbol{u}_0]$	$-(\boldsymbol{u}', \boldsymbol{\nabla} \cdot [\boldsymbol{u}'\, \boldsymbol{u}_0])_\Omega$	$-\left(\overline{\boldsymbol{u}'\, \boldsymbol{u}'} : \boldsymbol{\nabla}\, \boldsymbol{u}_0\right)_\Omega$	P
$-\boldsymbol{\nabla} \cdot [\boldsymbol{u}_0\, \boldsymbol{u}']$	$-(\boldsymbol{u}', \boldsymbol{\nabla} \cdot [\boldsymbol{u}_0\, \boldsymbol{u}'])_\Omega$	$-\left[\boldsymbol{u}_0\, \frac{1}{2}\overline{\|\boldsymbol{u}'\|^2}\right]_{\partial\Omega}$	$+C$
$-\boldsymbol{\nabla} \cdot [\boldsymbol{u}'\, \boldsymbol{u}']$	$-(\boldsymbol{u}', \boldsymbol{\nabla} \cdot [\boldsymbol{u}'\, \boldsymbol{u}'])_\Omega$	$-\left[\overline{\boldsymbol{u}'\, \frac{1}{2}\|\boldsymbol{u}'\|^2}\right]_{\partial\Omega}$	$+T$
$+\nu \triangle \boldsymbol{u}_0$	$+\nu\, (\boldsymbol{u}', \triangle \boldsymbol{u}_0)_\Omega$		
$+\nu \triangle \boldsymbol{u}'$	$+\nu\, \left(\overline{\boldsymbol{u}', \triangle \boldsymbol{u}'}\right)_\Omega$	$+\nu\, \left(\overline{\boldsymbol{u}' \cdot \triangle \boldsymbol{u}'}\right)_\Omega$	$+D$
$-\boldsymbol{\nabla} p$	$-(\boldsymbol{u}', \boldsymbol{\nabla} p)_\Omega$	$-\left[\overline{\boldsymbol{u}'\, p'}\right]_{\partial\Omega}$	$+F$

Table 4. Derivation scheme of the modal energy flow balance analog to Tab. 3 following the recipe of Tab. 1.

projection on $a_i \boldsymbol{u}_i$	Galerkin-representation	modal energy-flow balance (averaged)	do. (short form)
$(a_i \boldsymbol{u}_i, \partial_t \boldsymbol{u}')_\Omega =$	$\frac{d}{dt}\left(\frac{1}{2} a_i^2\right) =$	$dK_i/dt =$	do.
$-(a_i \boldsymbol{u}_i, \boldsymbol{\nabla} \cdot [\boldsymbol{u}_0\, \boldsymbol{u}_0])_\Omega$	$q^c_{i00} a_i$		
$-(a_i \boldsymbol{u}_i, \boldsymbol{\nabla} \cdot [\boldsymbol{u}'\, \boldsymbol{u}_0])_\Omega$	$+\sum_{j=1}^{N} q^c_{ij0} a_i a_j$	$+2 q^c_{ii0}\, K_i$	P_i
$-(a_i \boldsymbol{u}_i, \boldsymbol{\nabla} \cdot [\boldsymbol{u}_0\, \boldsymbol{u}'])_\Omega$	$+\sum_{j=1}^{N} q^c_{i0j} a_i a_j$	$+2 q^c_{i0i}\, K_i$	$+C_i$
$-(a_i \boldsymbol{u}_i, \boldsymbol{\nabla} \cdot [\boldsymbol{u}'\, \boldsymbol{u}'])_\Omega$	$+\sum_{j,k=1}^{N} q^c_{ijk} a_i a_j a_k$	$+\sum_{j,k=1}^{N} q^c_{ijk} \overline{a_i a_j a_k}$	$+T_i$
$+\nu\,(a_i \boldsymbol{u}_i, \triangle \boldsymbol{u}_0)_\Omega$	$+\nu l_{i0} a_i$		
$+\nu\,(a_i \boldsymbol{u}_i, \triangle \boldsymbol{u}')_\Omega$	$+\nu \sum_{j=0}^{N} l_{ij} a_i a_j$	$+2\nu l_{ii} K_i$	$+D_i$
$-(a_i \boldsymbol{u}_i, \boldsymbol{\nabla} p)_\Omega$	$+\sum_{j,k=0}^{N} q^p_{ijk} a_i a_j a_k$	$+\sum_{j,k=0}^{N} q^p_{ijk} \overline{a_i a_j a_k}$	$+F_i$

3.3 Finite-time thermodynamics as closure model

In the following, we propose a closure for the first and second moments of a Galerkin system, inspired by finite-time thermodynamics (FTT) (Andresen, 1983). The modal balance equation for momentum and for energy constitute consistency conditions for Galerkin modeling process. The FTT closure of these equations can provide further insights and make predictions. These predictions may include intermodal dependencies, the behavior of a reduced system, auxiliary terms needed for the reduced system, a good way to aggregate mode groups in single 'quasi modes', or transient behavior.

The consideration of transients may require the inclusion of non-POD modes in the Galerkin model. Hence, we formulate the closure for general orthogonal modes. The general Reynolds decomposition of the mode

amplitudes read

$$a_i = m_i + a_i', \quad m_i := \langle a_i \rangle, \quad K_i = \langle (a_i')^2 \rangle / 2. \tag{46}$$

The closure shall determine the mean values m_i and fluctuation levels K_i, both for $i = 1, \ldots, N$. We exploit the energy preservation of the quadratic Galerkin-system term (Kraichnan and Chen, 1989). The main closure assumptions are that the i-th external energy flow is only a function of the i-th energy, $Q_i = Q_i(K_i)$ and that the triadic interaction is only a function of the involved modal energies $T_{ijk} = T_{ijk}(K_i, K_j, K_k)$, i.e. not higher or lower moments.

The FTT modeled modal Reynolds and modal TKE equations read

$$\dot{m}_i = c_i + \sum_{j=1}^{N} l_{ij}\, m_j + \sum_{j,k=1}^{N} q_{ijk}\, m_j\, m_k + \sum_{j=1}^{N} 2 q_{ijj}\, K_j, \tag{47a}$$

$$\dot{E}_i = Q_i + T_i, \quad \text{where} \quad Q_i = q_i K_i, \quad T_i = \sum_{j,k=1}^{N} T_{ijk}, \tag{47b}$$

$$q_i = \chi_i + \sum_{j=1}^{N} \chi_{ij}\, m_j, \tag{47c}$$

$$T_{ijk} = \alpha \chi_{ijk} \sqrt{K_i K_j K_k} \left(1 - \frac{3K_i}{K_i + K_j + K_k} \right), \tag{47d}$$

where χ_i, χ_{ij} and χ_{ijk} are functions of the Galerkin system coefficients and α is derived from an energetic consistency condition. For the details, the reader is referred to the original publications (Noack et al., 2008, 2010).

Note that (47) represent $2N$ equations for $2N$ unknowns. The FTT framework (47) includes, for instance, the amplitude equations for transient and post-transient behavior of generalized mean-field models with one or more incommensurable frequencies (Noack et al., 2003; Luchtenburg et al., 2009a). Another implication is the absolute equilibrium ensemble (Lesieur, 1993) for Hamiltonized equations. In other words, a condition for equipartition of energy between the modes is defined.

The statistical moments m_j and K_j are searched as the fixed point of the equation (47). Currently, the closure has been successfully applied to a mathematical Galerkin model of the modified Burgers' equation, a POD model of the cylinder wake, and a physical Galerkin model mimicking homogeneous turbulence (Noack et al., 2008). More applications of this closure are actively pursued by the authors.

4 Auxiliary models as key enablers

In previous sections, we have outlined the POD Galerkin method (§2) and associated balance equations (§3). More often than not this method may fail to yield robust, control-oriented models. Root causes are the lack of completeness of POD modes or the intended compression of the physics into few modes. This section shall serve as trouble shooting guide, showing physics-based generalizations of the Galerkin expansion and helpful modifications of the Galerkin system.

First (§4.1), the main challenges are enumerated. Cures are presented in form of general modeling principles addressing the root causes of the challenges. In the following, these principles are detailed as enablers for the Galerkin expansion (§4.2), for the natural dynamics (§4.3), and for the actuation effect (§4.4).

4.1 Challenges and modeling principles

Mathematical Galerkin models can be proven to converge to the Navier-Stokes solution with increasing mode number under suitable conditions (Ladyzhenskaya, 1963). The POD expansion can be expected to converge against the original data in averaged L_2 sense. However, the corresponding hierarchy of Galerkin systems may fail to resolve the Navier-Stokes equation in important aspects. Moreover, the kinematic resolution of the POD expansion may become unsuitable away from the design condition, e.g. at another Reynolds number or with actuation applied. The reason of these challenges can be traced back to the generic incompleteness of the POD in $L^2(\Omega)$.

Incompleteness of POD may lead to following challenges of the corresponding Galerkin method:

1. If the Navier-Stokes solution depends sensitively on small variations of the configuration or the initial condition, the model solution can be expected to be correspondingly strongly effected by modeling errors, even for direct numerical simulations. In the sequel, we assume that the flow dynamics is robust, i.e. we can target a robust reduced-order model as well.
2. The stability property of the Navier-Stokes solution is not conserved during Galerkin projection, even if the Galerkin expansion is 100% accurate. A stable Navier-Stokes solution may lead to an unstable Galerkin solution or the other way round. Simple 3-dimensional models reveal that the omission of a single non-energetic mode may drastically change the stability property of the remaining dynamics (Rempfer, 2000; Noack et al., 2003). Even worse, mean-field models

show that low-energy mean-field modes (shift-modes) lead to cubic stabilizing terms in the Galerkin system (Aubry et al., 1988; Ukeiley et al., 2001; Podvin, 2009), i.e. cannot be cured by re-calibrating the constant, linear or quadratic term.

3. The solution of the Navier-Stokes equation will be a solution of the Galerkin model if the Galerkin basis is accurate. But the Galerkin system may have more unphysical solutions (Rempfer, 1995; Noack et al., 2003). In other words, the Galerkin system may have a narrow region of validity, possibly only the attractor.
4. Turbulent flows are by definition high-dimensional and the Galerkin model shall by construction resolve only the gist, the coherent structures. These structures may contain only a fraction of the turbulent kinetic energy, say 20–50% in case of highly visible coherency. Hence, the effect of the Galerkin expansion residual on the dynamics cannot be ignored and must be modeled. The general recipe to resolve 90% of the fluctuation energy is typically not doable and misses the very goal of reduced-order models.
5. The purpose of actuation is generally to change the coherent structures not only in amplitude but also in shape. One example is to delay vortex shedding behind a bluff body further downstream. Hence, the application of control may invalidate the Galerkin model design at natural conditions.
6. Local small-scale actuation may distort coherent structures from small to large-scale structures. This multi-scale effect can generally not be resolved in the standard POD Galerkin method — like in unsteady RANS methods as well.

The challenges look intimidating. A rich kaleidoscope of seemingly unrelated cures can be found for numerous individual configurations. Fortunately, the root causes for ailing POD models can easily be explained and can often be cured by corresponding simple principles. We mentally partition the flow in coherent structures with characteristic dominant frequency ω_c, a base flow with slow variations $\omega \ll \omega_c$, and small-scale stochastic turbulent fluctuations at high frequencies $\omega \gg \omega_c$. By construction, the POD model may well resolve the coherent structures and associated instabilities and nonlinearities. The coherent structures are continually 'nurtured' by the mean flow. The energy growth is limited by base flow variations and by the turbulence cascade, i.e. by the low- and high-frequency side of the spectrum. By construction, a POD model will fail to resolve the turbulence cascade as energy sink and is not guaranteed to resolve stabilizing base flow variations. Hence, the Galerkin model will be much stabler if the POD bases is augmented by additional modes for the base flow variations and a

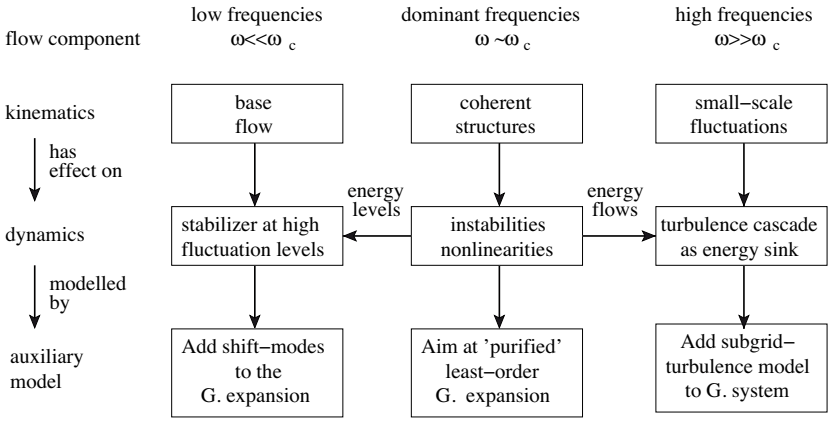

Figure 1. Simplified flow physics and modeling principles. 'G.' stands for Galerkin. The figure is explained in the text.

good auxiliary model for unresolved fine-scale turbulence. Fig. 1 summarizes these principles. In other words, there is no reason to hope for a stable Galerkin model if the physical stabilizing effects are not resolved. Historically, the first pioneering POD model by Aubry et al. (1988) includes a base flow model and an auxiliary turbulence model, i.e. is consistent with these recipes.

4.2 Generalizations of the Galerkin expansion

We outline generalizations of the POD expansion, derived from the evolution equation or resolving multiple operating conditions. First (§4.2), a simple example demonstrates how the evolution equation can be used to construct a dynamically important missing mode. Sections §4.2 and §4.2 address fluctuations with one varying frequency or multiple incommensurable frequencies. Finally (§4.2), general approaches are enumerated.

Shift mode For reasons of simplicity, we consider a simple system of ordinary differential equation illustrating the dynamic incompleteness of POD and showing a necessary cure. This system is derived from the Navier-Stokes equation under assumptions of mean-field theory, i.e. the soft onset

of an oscillatory fluctuation (Noack et al., 2003):

$$\begin{aligned} \dot{u} &= (\sigma_1 - \beta w)\, u - (\omega_1 + \gamma w)\, v && \text{(48a)} \\ \dot{v} &= (\sigma_1 - \beta w)\, v + (\omega_1 + \gamma w)\, u && \text{(48b)} \\ \dot{w} &= -\sigma_\Delta\, w + \alpha\, \left(u^2 + v^2\right) && \text{(48c)} \end{aligned}$$

The roles of the parameters $\sigma_1 > 0$, $\sigma_\Delta > 0$, $\alpha > 0$, $\beta > 0$, and γ are described below. The flow of (48) is illustrated in a phase portrait (Fig. 2). The dynamic behavior is easily inferred from a transcription to cylindrical coordinates r, θ, where $r\, e^{\imath\theta} = u + \imath v$, $\imath = \sqrt{-1}$ being the imaginary unit:

$$\begin{aligned} \dot{r} &= (\sigma_1 - \beta w)\, r, && \text{(49a)} \\ \dot{\theta} &= (\omega_1 + \gamma w)\,, && \text{(49b)} \\ \dot{w} &= -\sigma_\Delta\, w + \alpha\, r^2. && \text{(49c)} \end{aligned}$$

We introduce $\boldsymbol{u} = [u, v, w]^\top$. Evidently, $\boldsymbol{u}_s = 0$ is the unstable fixed point of the system (48). The neighboring infinitesimal fluctuation spirals outwards in the $w = 0$ plane with growth rate σ_1 and frequency ω_1. The fluctuation level r^2 shifts the stable mean flow parameter w away from the origin. Typically, the mean flow immediately adjusts to the fluctuation level (Noack et al., 2003; Tadmor and Noack, 2004), $\sigma_\Delta \gg \sigma_1$, showing the slaving to the parabolic mean-field manifold,

$$w = \frac{\alpha}{\sigma_\Delta}\, r^2. \tag{50}$$

This slaving (Haken, 1983) in (49a), (49b) yields the famous Landau equations for the onset of a supercritical Hopf bifurcation:

$$\dot{r} = \sigma_1 r - \beta^\star r^3, \quad \dot{\theta} = \omega_1 + \gamma^\star r^2, \tag{51}$$

with $\beta^\star = \alpha\beta/\sigma_\Delta$ and $\gamma^\star = \alpha\gamma/\sigma_\Delta$. As a result of changing w, the growth rate (frequency) is reduced (changed) via the β (γ) term. Saturation happens at $\dot{r} = 0$ or, equivalently, at fluctuation level r_∞^2, height w_∞ and frequency ω_∞ given by

$$r_\infty^2 = \frac{\sigma_1\, \sigma_\Delta}{\alpha\, \beta}, \quad w_\infty = \frac{\sigma_1}{\beta} \quad \omega_\infty = \omega_1 + \frac{\sigma_1 \gamma}{\beta} \tag{52}$$

The periodic solution reads

$$\boldsymbol{u} = \boldsymbol{u}_0 + a_1\, \boldsymbol{u}_1 + a_2\, \boldsymbol{u}_2, \tag{53}$$

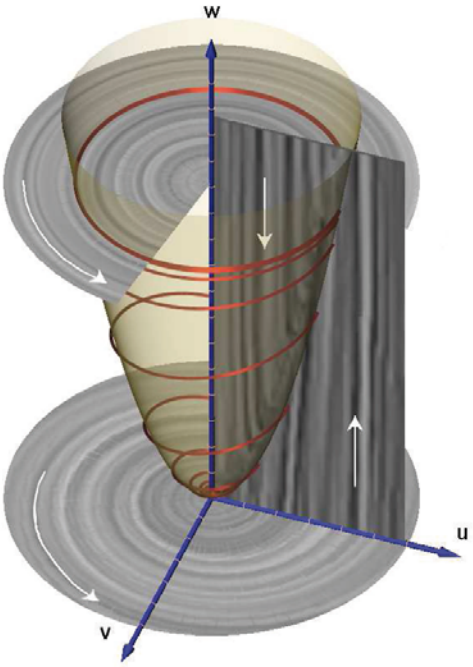

Figure 2. Phase portrait of (48). The red curve shows a transient from the unstable fixed point to the stable limit cycle on the mean-field paraboloid which is indicated by a semi-transparent surface. In the planes, the tangential flow component is visualized. Selected white arrows indicate the direction of the flow. The lower (middle) plane contains the fixed point (limit cycle). The half-plane $v = 0, u > 0$ displays the transient towards the mean-field paraboloid.

where $\boldsymbol{u}_0 = [0, 0, w_\infty]^\top$ represents the mean, and $\boldsymbol{u}_1 = [1, 0, 0]^\top$, $\boldsymbol{u}_2 = [0, 1, 0]^\top$, $a_1 = r_\infty \cos \omega_\infty t$, $a_2 = r_\infty \sin \omega_\infty t$ the harmonic oscillation modulo a phase shift. Not incidentally, (53) is the exact POD of the limit cycle with $\boldsymbol{u}_1$ and $\boldsymbol{u}_2$ as POD modes and $\lambda_1 = \lambda_2 = r_\infty^2/2$ as eigenvalues. A straight-forward Galerkin projection of the mean-field system (48) on these 2 POD modes yields a marginally stable center

$$\dot{a}_1 = -a_2 \quad \dot{a}_2 = a_1. \tag{54}$$

The Galerkin system (54) illustrates the challenges 2 and 3 of §4.1. The limit cycle is stable in the original 3-dimensional system (48), but only marginally stable in the POD system (54). The POD system contains the periodic solution (53), but also a continuum of unphysical solutions. The truncated dynamics do not resolve the amplitude selection mechanism on the mean-field paraboloid (50) described by the cubic (!) Landau equation (51).

From this example, we can easily infer possible cures for the poorly performing POD Galerkin method. We kinematically include the steady solution in (53) by adding $a_3\boldsymbol{e}_3$ to the expansion, i.e. the direction from steady solution $\boldsymbol{u}_s$ to the mean flow $\boldsymbol{u}_0$. Thus, we restore the full dynamics and associated damping mechanism. The direction may be called *shift-mode* as it shifts the center of the attractor (here: limit cycle). The shift-mode from the mean flow $\boldsymbol{u}_0$ and steady solution $\boldsymbol{u}_s$ is normalized:

$$\boldsymbol{u}_\Delta = \frac{\boldsymbol{u}_0 - \boldsymbol{u}_s}{\|\boldsymbol{u}_0 - \boldsymbol{u}_s\|_\Omega}. \tag{55}$$

We assume orthogonality with the POD modes, or enforce orthogonality with a Gram-Schmidt orthonormalization.

The steady unstable Navier-Stokes solution may be difficult to compute. Hence, we search for another approach. Reynolds-averaging of (48) yields only one nontrivial equation, namely the average of the third equation (49c)

$$0 = \sigma_\Delta\, \overline{w} + \alpha\, \overline{r^2}.$$

From this equation, we see that a change in the fluctuation level $\overline{r^2}$ immediately affects $\overline{w}$, i.e. shifts the limit cycle 'up' or 'down' in $\boldsymbol{e}_3$ direction. This dynamic consideration also indicates that $\boldsymbol{e}_3$ is an important direction to be included in the generalized POD expansion. The pendant for the Navier-Stokes discussion is the Reynolds equation and POD decomposition of the Reynolds stress tensor:

$$\boldsymbol{\nabla}\cdot(\boldsymbol{u}_0\boldsymbol{u}_0) = -\boldsymbol{\nabla}p_0 + \nu\triangle\boldsymbol{u}_0 - \boldsymbol{\nabla}\cdot\left(\sum_{i=1}^{\infty}\lambda_i\,\boldsymbol{u}_i\,\boldsymbol{u}_i.\right) \tag{56}$$

Evidently, $\boldsymbol{u}_0$ varies with changes in each eigenvalue λ_i. This ansatz is elaborated and exploited by Morzyński et al. (2006); Tadmor et al. (2010). For nominally 1-dimensional channel, Couette, or mixing layer flows, the Reynolds equation (56) can be solved directly (Aubry et al., 1988; Ukeiley et al., 2001; Podvin, 2009). The slaving between mean-flow modes and fluctuations leads to cubic terms, like in the Landau equation as an especially simple slaving example.

Deformable oscillatory modes In this section, we address a root cause of the frequently observed narrow dynamic bandwidth of POD models, outlined first by Deane et al. (1991). Let us consider a 1-dimensional, slowly spatially decaying traveling wave

$$u(x,t) = e^{-x/100}\,\cos\left[\kappa x - t\right], \quad x \geq 0, t \geq 0 \tag{57}$$

with wave number $\kappa > 0$ and unit circular frequency. We keep the discussion at a qualitative level. The analytics is presented in Noack (2006); Luchtenburg et al. (2009b). This wave motion is spanned by 2 POD modes $u^{\kappa}_{1,2}$ of similar energy.

$$u(x,t) = a_1(t)u^{\kappa}_1(x) + a_2(t)\,u^{\kappa}_2(x). \tag{58}$$

This POD is an exact representation for the chosen wave number, say $\kappa = 1$ but quickly deteriorates if κ is slightly, say 10%, of.

Suppose we want to capture a slow transient as κ increases from 1 to 1.5. A first idea may be a 4-dimensional expansion with POD mode pairs at $\kappa = 1$ and $\kappa = 1.5$, targeting a resolution at intermediate wavenumbers. However, superposition leads to an unphysical beat phenomena. A well resolving POD of the transient requires a large number of modes. Examples of this type are POD modes of the cylinder wake under chirp forcing (Bergmann et al., 2005). This large POD basis may lead to suitable models targeting full-information control (Bergmann et al., 2005), i.e. when state estimation is not an issue. For robust sensor-based control, the preservation of least-order representation is a must, since each state space direction can act as noise amplifier.

Strategies to preserve the least-order expansion (58) for variable parameter κ are abundantly offered in literature, mostly for the cylinder wake. A straight-forward example is a look-up table with a 'stack' of expansions at different κ and κ-estimator (Lehmann et al., 2005). Double POD (see the chapter of S. Siegel in this volume) follows a similar logic. Continuous mode (Morzyński et al., 2007) and geodesic interpolation are continuous interpolation variants.

Tracking mode changes is crucial if the model-based control is based on sensors and actuators at different locations (Gerhard et al., 2003), i.e. if POD modes communicate phase differences between input and output. In some cases, slow variations of frequencies and wavenumbers can or shall be ignored in the POD model, e.g. if only the near-wake region is of interest. In this case, POD-based phase averaging techniques (Depardon et al., 2007) can be employed.

Modes for different frequencies Some flows display simultaneously two or more distinct oscillatory structures at different locations. One example is high-frequency forcing to mitigate von Kármán vortex shedding (Thiria et al., 2006; Pastoor et al., 2008). In this case, modes based on extraction of pure frequencies are desirable. Numerous straight-forward techniques are available. Examples are frequency filtering, phase-averaging for natural flow, or linear stochastic estimation (Bonnet et al., 1998) connecting the flow to actuation signal. Corresponding 4-dimensional models for flows with two dominant frequencies have been used for open- and closed-loop control of wakes (Luchtenburg et al., 2010) and flow around airfoils (Luchtenburg et al., 2009a).

General approaches Here, we discuss generalizations of POD comprising multiple operating conditions. Consider, for instance, a flow actuated at 5 different frequencies.

A POD of all operating conditions may be obtained by putting all snapshots in the same 'basket', i.e. performing POD from this enlarged data set. This approach has severe drawbacks: (1) The weighting of each operating condition depends on the number and energy of the individual snapshots at each operating condition. (2) There is no guaranteed minimal resolution at each operating condition. (3) The POD may show unphysical beat phenomena (see §4.2) or the number of modes is unnecessarily large.

Sequential POD (Jørgensen et al., 2003) addresses the first two drawbacks. Here, a minimal resolution at all operating conditions is prescribed. In the first iteration, POD resolves the first data ensemble at prescribed accuracy. In the second iteration, POD modes are added based on the residual of the first expansion with respect to second data ensemble. The new enlarged data set has prescribed accuracy at the first two operating conditions. The procedure is continued until all operating conditions are included.

The mentioned POD generalizations assume given 'off-line' data. Elegant 'online' corrections of POD bases during a simulation or an experiment are obtained with a trust-region (TR) approach (Fahl, 2000; Bergmann and Cordier, 2008). This POD-TR approach is well aligned with the search for least-order representations.

4.3 Modeling natural dynamics

In this section, we model the effect of unresolved fluctuations in the Galerkin system. Periodic flows may be fully resolved by 4 to 10 modes (Deane et al., 1991; Noack et al., 2003, 2005). Transitional flows may require

thousands of modes for a 90% resolution of turbulent kinetic energy (TKE) and a much smaller percentage of the dissipation. The number of modes for fully turbulent flows may be estimated by the Kolmogorov dimension $N \sim Re^{9/4}$ (see, e.g., Landau and Lifshitz (1987)).

The computational load for one time-step integration of a Galerkin system (28) increases with N^3 due to the quadratic term, while the load of grid-based Navier-Stokes solvers increases only linearly with the number of grid points. This limits the practicality of the Galerkin method to $N \sim 100$ or $N \sim 1000$. Robust sensor-based control design poses more severe restrictions on the dimension, say $N \sim 10$. Hence, the Galerkin expansion with N modes will have a non-negligible residual $\delta\boldsymbol{u}$ for most non-periodic flows:

$$\boldsymbol{u} = \boldsymbol{u}_0 + \sum_{i=1}^{N} a_i \boldsymbol{u}_i + \delta\boldsymbol{u}, \quad \text{where} \quad \delta\boldsymbol{u} = \sum_{i=N+1}^{\infty} a_i \boldsymbol{u}_i. \tag{59}$$

The error $\delta\boldsymbol{u}$ leads to a corresponding propagator residual δf_i in the dynamical system (28)

$$\dot{a}_i = c_i + \sum_{j=1}^{N} l_{ij}\, a_j + \sum_{j,k=1}^{N} q_{ijk}\, a_j\, a_k + \delta f_i, \tag{60a}$$

$$\delta f_i = \sum_{j=N+1}^{\infty} l_{ij}\, a_j + \sum_{\substack{j,k=1 \\ \max\{j,k\}>N}}^{\infty} q_{ijk}\, a_j\, a_k. \tag{60b}$$

Model development for δf_i is guided by the picture that first N modes represent low to dominant frequencies $\omega \lesssim \omega_c$. while the residual describes large frequencies $\omega \gg \omega_c$. The linear term of δf_i in (60b) contributes with higher frequencies in (60a) and can loosely be interpreted as noise. The quadratic term of δf_i in (60b) will show the whole frequency spectrum.

First, we estimate the average of the propagator residual from the Galerkin-Reynolds equation (39)

$$0 = c_i + \underbrace{\sum_{j=1}^{N} 2q_{ijj}K_j}_{resolved} + \underbrace{\sum_{j=N+1}^{\infty} 2q_{ijj}K_j}_{from\ \delta f_i}. \tag{61}$$

The last term can be considered negligible with respect to the middle term, assuming that the coherent structures resolved by N modes characterize the Reynolds-stress tensor.

Secondly, we investigate the energetic effect of the propagator residual and make the ansatz $\delta f_i = d_i a_i$. From turbulence theory, we expect a

dissipative effect of the small-scale structures, i.e. a negative growth rate d_i. The modal energy equation (45) implies for (60b) following consistency condition for the modal power $\overline{a_i \delta f_i}$

$$2d_i K_i = \sum_{\substack{j,k=1 \\ \max\{j,k\}>N}}^{\infty} q_{ijk}\, \overline{a_i\, a_j\, a_k}. \tag{62}$$

Note that the linear term of the propagator residual does not contribute to that balance. On the attractor, (62) defines a unique (constant) value d_i^∞.

Rempfer and Fasel (1994) reason that the propagator residual has a similar effect than a 'modal eddy viscosity' ν_i^T, i.e. $\delta f_i = \nu_i^T \sum_{j=0}^{N} l_{ij}^\nu a_j$, following the very ideas of Boussinesq, Prandtl and Smagorinsky adopted in computational fluid mechanics. The value ν_i^T is obtained from the modal TKE equation. This ansatz yields $d_i = \nu_i^T l_{ii}^\nu$. In fact, most authors employ a linear term representing the nonlinear effect of small-scale turbulence. This ansatz appears to works well for small-bandwidth dynamics, e.g. laminar and transitional flows, without additional stabilizers.

For broadband turbulence, diverging Galerkin solutions are frequently observed (yet rarely published). One reason can be attributed to the fact that the nonlinearities have a stronger damping effect at high fluctuation levels than the postulated linear term. We estimate the correct scaling by assuming that the modal energies $K_i = \kappa_i K$ have a constant non-negative share $\kappa_i \geq 0$ in the total TKE K. Here, $\sum_{i=1}^{N} \kappa_i = 1$ and K is considered as a free parameter. The right-hand side of (62) can be approximated with the FTT closure equation (47d). Thus, (62) becomes after division by $2\kappa_i K$

$$d_i = \frac{1}{2\kappa_i} \left[\sum_{\substack{j,k=1 \\ \max\{j,k\}>N}}^{\infty} \alpha \chi_{ijk} \sqrt{\kappa_i \kappa_j \kappa_k} \left(1 - \frac{3\kappa_i}{\kappa_i + \kappa_j + \kappa_k} \right) \right] K^{1/2}.$$

The term in the square brackets is independent of K. Hence, this equation implies that the growth-rate d_i scales with $K^{1/2}$. In other words, the identified attractor value d_i^∞ should be corrected with a corresponding factor

$$d_i = d_i^\infty \sqrt{\frac{K}{K^\infty}}, \tag{63}$$

where K^∞ is total TKE on the Navier-Stokes attractor. In practice and without loss of generality, K can be assumed to be the resolved fluctuation energy. A POD model of a turbulent jet (Schlegel et al., 2009) was found to be stable when using the new scaling (63) and diverging during some

corona bursts when assuming a constant value. Similarly, an FTT-based eddy viscosity (Noack et al., 2010) is derived for periodic flows leading to $d_i \sim K$ scaling. The ad-hoc reasoning leading to (63) may be subject to numerous concerns and refinements. At minimum, a new potential direction for future 'subgrid' turbulence representations δf_i is offered.

4.4 Modeling actuation effects

We derive the forcing term in Galerkin system (27) for volume force actuation §4.4 and for boundary actuation §4.4. Finally (§4.4), a recipe is given for identifying a forcing term from data.

Volume force actuation The flow may actuated with volume force. Examples are magnetohydrodynamic (MHD) forces, the buoyancy term in the Boussinesq approximation, and fictitious forces from choosing a body-fixed coordinate system of a moving body.

In general, the volume force can be expressed or approximated by a modal expansion in space-dependent carrier fields $\boldsymbol{g}_i$ and time-dependent actuation amplitudes b_i.,

$$\boldsymbol{g}(\boldsymbol{x},t) = \sum_{i=1}^{N_V} b_i(t)\, \boldsymbol{g}_i(\boldsymbol{x}). \tag{64}$$

The Galerkin representation for $N_V = 1$ is derived in §2.4. For larger number of volume force modes N_V, superposition yields

$$\dot{a}_i = f_i(\boldsymbol{a}) + \sum_{j=1}^{N} g_{ij} b_j, \tag{65}$$

where f_i is the propagator for the unactuated dynamics and $g_{ij} := (\boldsymbol{u}_i, \boldsymbol{g}_j)_\Omega$ are the gains from the volume force modes.

Boundary actuation The flow may be manipulated with suction and blowing at the boundary $\partial\Omega$. Contrary to the stationary boundary condition (3), we now impose a time-dependent velocity. A Galerkin-type expansion with N_A modes shall represent this distribution,

$$\boldsymbol{u}_{BC}(\boldsymbol{x},t) = \sum_{i=-N_A}^{-1} a_i(t)\, \boldsymbol{u}_i(\boldsymbol{x}), \quad \boldsymbol{x} \in \partial\Omega. \tag{66}$$

Here, $\boldsymbol{u}_i$ may characterize the exit profile of a local actuator and a_i denotes the amplitude. Straightforward POD Galerkin method will slave actuation

and flow dynamics, i.e. the actuation is reconstructed from the Galerkin system. One example is a Galerkin model for the Kelvin-Helmholtz vortices excited by a stability eigenmode at the inlet (Noack et al., 2005). The Galerkin model 'sees' that only one actuation is consistent with the POD and Navier-Stokes equation. The same observation applies to any Galerkin model on subdomains with inflow and outflow.

However, a straight-forward Galerkin projection will not reveal the effect of this forcing as free input, since only a zero-set of the whole domain is affected. This input can be 'freed' as follows. (66) is generalized for the whole domain Ω by introducing incompressible actuation modes $\boldsymbol{u}_i$, $i<0$,

$$\boldsymbol{u}^{[-N_A..-1]}(\boldsymbol{x},t)=\sum_{i=-N_A}^{-1} a_i(t)\,\boldsymbol{u}_i(\boldsymbol{x}). \tag{67}$$

(66) and (67) coincide on the boundary. The choice of the actuation mode is largely a design parameter. One example is a potential vortex representing rotations of a circular cylinder (Bergmann et al., 2005). A more general strategy is offered by Kasnakoglu et al. (2008). Now, POD retaining N modes is performed on the remainder $\boldsymbol{u}-\boldsymbol{u}^{[-N_A..-1]}$. The resulting expansion reads

$$\boldsymbol{u}(\boldsymbol{x},t)=\sum_{i=-N_A}^{N} a_i(t)\,\boldsymbol{u}_i(\boldsymbol{x}). \tag{68}$$

Note that $a_0\equiv 1$, a_i with $i<0$ are predetermined actuation amplitudes and a_i with $i>0$ represent POD mode amplitudes. (68) fulfills exactly the incompressibility condition *(GM1)* and the new unsteady boundary conditions for any choice of the a_i, $i>0$ *(GM2)* of §2.2.

Galerkin projection of (1b) on (68) yields

$$\dot{a}_i=\nu\sum_{j=-N_A}^{N} l_{ij}^{\nu}\,a_j+\sum_{j,k=-N_A}^{N}\left(q_{ijk}^{c}+q_{ijk}^{p}\right)\,a_j\,a_k-\sum_{j=-N_A}^{-1} m_{ij}\dot{a}_j. \tag{69}$$

The terms of dynamical system generalize (27) by a larger index set of modes. The last new term with the mass matrix $m_{ij}=(\boldsymbol{u}_i,\boldsymbol{u}_j)_\Omega$, $i>0$, $j<0$ arises from the local acceleration term and the non-orthonormality between actuation and POD modes.

POD Galerkin models with actuation modes have been constructed for wakes behind rotating (Graham et al., 1999; Bergmann et al., 2005), oscillating circular cylinders (Noack et al., 2004), and local actuation (Weller et al., 2009).

Identification of a forcing term In aerodynamic flow control applications, small actuators may effect large-scale coherent structures. In principle, such actuation can be derived from a priori consideration. In practice, a low-order Galerkin model is expressly designed to ignore the kinematics of small-scale phenomena. For the effect on the large-scale dynamics, a forcing term needs to be identified. The *structure identification* of the analytical form of this term may be based on the Navier-Stokes equation. The *parameter identification* utilizes available data.

In the sequel, we outline a simple identification technique which has been employed in a number of turbulence control studies with periodic forcing (Luchtenburg et al., 2009a, 2010; John et al., 2010). Let f_i be the propagator of the natural dynamics and b be the amplitude of a local actuator. Then, we postulate a forced system of the form

$$\dot{a}_i = f_i(\boldsymbol{a}) + g_{1i} b + g_{2i} \dot{b}. \tag{70}$$

This form can be derived from a priori considerations (Luchtenburg et al., 2009a). The forcing term may be considered as two pseudo volume forces. The last term with $\dot{b}$ is often neglected but nevertheless important. This term allows the actuation b to 'hit' each mode with the right phase. The gains can be inferred from the mode amplitudes $t \mapsto \boldsymbol{a} = \boldsymbol{a}^a$ and control $t \mapsto b$ of the reference simulation or experiment with actuation. Substituting this actuated solution in (70), multiplication with b or $\dot{b}$, averaging, and exploiting $\overline{b\,\dot{b}} = 0$ for long time intervals yields the formula for the gains:

$$g_{1i} = \overline{(\dot{a}_i^a - f_i(\boldsymbol{a}^a))\, b} / \overline{b^2}, \tag{71a}$$

$$g_{2i} = \overline{(\dot{a}_i^a - f_i(\boldsymbol{a}^a))\, \dot{b}} / \overline{\dot{b}^2}. \tag{71b}$$

For periodic actuation $b = B\cos\omega^a t$, this procedure implies dynamical system consistency with respect to the first actuated harmonics, i.e. projections on $\cos\omega^a t$ and $\sin\omega^a t$.

5 Conclusions and Outlook

We have outlined the mathematical frame-work for reduced-order Galerkin models, particularly for empirical variants based on POD. In §2, we elaborated a standard operating procedure. This should allow an interested reader to build a corresponding model for his/her data. Important physics insights for modeling and control are gained from refined statistical analyses of the Navier-Stokes equation, as outlined in §3. In §4, we have attempted to give a trouble shooting guide for ROM of turbulent flows and its control. This guide starts with physical mechanisms which may not be resolved

for a particular configuration and ends with recipes which have proven to work for many cases. The next chapter by G. Tadmor et al. will outline applications for nonlinear laminar wake stabilization.

Reduced-order modeling is under rapidly evolving development in an increasing number of institutes involving more and more interdisciplinary research initiatives. Its potential is far from being exploited. The low dimension of the Galerkin model makes it

- an ultimate testbed of the gained physical understanding,
- a link to nonlinear dynamics analyses,
- a numerically tractable framework for mathematical turbulence theory,
- a necessity for many control designs, and
- an exciting door-opener to many system-reduction methods of theoretical physics.

Current turbulence control applications indicate a pressing need for understanding the nonlinearities of the turbulence cascade and actuation effects — transcending the current possibilities of available knowledge. ROM offer an ideal plant for these investigations (Luchtenburg et al., 2010).

As word of warning, we mention that the Galerkin method is an essentially elliptic approach for often hyperbolic Navier-Stokes dynamics. The very ansatz, the Galerkin expansion with global modes, assumes a globally synchronized flow dynamics. This may be a good approximation of internal flows or of the neighborhood of a recirculation bubble in open flows. On contrary, the Galerkin model is not well suited for transient shear flows with nearly uni-directional 'hyperbolic' convection of vortices (Noack et al., 2005). A cure may be provided in form of local modes or coupled Galerkin models. As alternative, vortex methods (Cottet and Koumoutsakos, 2000; Pastoor et al., 2008) provide more robust reduced-order models. However, the hybrid nature of vortex models challenges control design methods due to continuous injection, removal or merging of states (vortices).

Bibliography

K. Afanasiev. *Stabilitätsanalyse, niedrigdimensionale Modellierung und optimale Kontrolle der Kreiszylinderumströmung (transl.: Stability analysis, low-dimensional modelling, and optimal control of the flow around a circular cylinder).* PhD thesis, Fakultät Maschinenwesen, Technische Universität Dresden, 2003.

E. Åkervik, J. Hœpffner, U. Ehrenstein, and D. S. Henningson. Optimal growth, model reduction and control in separated boundary-layer flow using global eigenmodes. *J. Fluid Mech.*, 579:305–314, 2007.

B. Andresen. *Finite-Time Thermodynamics*. Physics Laboratory II, University of Copenhagen, Copenhagen, 1983.

N. Aubry, P. Holmes, J. L. Lumley, and E. Stone. The dynamics of coherent structures in the wall region of a turbulent boundary layer. *J. Fluid Mech.*, 192:115–173, 1988.

P. F. Batcho. *Global Spectral Methods for the Solution of the Incompressible Navier-Stokes Equations in Complex Geometries: The Generalized Stokes Eigensystem*. PhD thesis, Princeton University, 1994.

M. Bergmann and L. Cordier. Optimal control of the cylinder wake in the laminar regime by Trust-Region methods and POD Reduced Order Models. *J. Comp. Phys.*, 227:7813–7840, 2008.

M. Bergmann, L. Cordier, and J.-P. Brancher. Optimal rotary control of the cylinder wake using proper orthogonal decomposition reduced order model. *Phys. Fluids*, 17:097101–1. . .21, 2005.

J.-P. Bonnet, D.R. Cole, J. Delville, M. N. Glauser, and L. S. Ukeiley. Stochastic estimation and proper orthogonal decomposition — complementary techniques for identying structure. *Exp. Fluids*, 17:307–314, 1998.

F. H. Busse. Numerical analysis of secondary and tertiary states of fluid flow and their stability properties. *Appl. Sci. Res.*, 48:341–351, 1991.

L. Cordier and M. Bergmann. Proper orthogonal decomposition: An overview. In P. Millan and M.L. Riethmuller, editors, *Post-Processing of Experimental and Numerical Data*, VKI Lecture Series 2003-03. Von Kármán Institut for Fluid Dynamics, 2003.

L. Cordier, B. Abou El Majd, and J. Favier. Calibration of POD reduced-order models by Tikhonov regularization. *Internat. J. Numer. Meth. Fluids*, 63(2), 269–296, 2010.

G. H. Cottet and P. Koumoutsakos. *Vortex Methods — Theory and Practice*. Cambridge University Press, Cambridge, 2000.

A. E. Deane, I. G. Kevrekidis, G. E. Karniadakis, and S. A. Orszag. Low-dimensional models for complex geometry flows: Application to grooved channels and circular cylinders. *Phys. Fluids A*, 3:2337–2354, 1991.

S. Depardon, J. J. Lasserre, L. E. Brizzi, and J. Borée. Automated topology classification method for instantaneous velocity fields. *Exp. Fluids*, 42: 697–710, 2007.

M. Fahl. *Trust-region methods for flow control based on reduced order modeling*. PhD thesis, Universität Trier, 2000.

C. A. J. Fletcher. *Computational Galerkin Methods*. Springer, New York, 1st edition, 1984.

G. Galletti, C. H. Bruneau, L. Zannetti, and A. Iollo. Low-order modelling of laminar flow regimes past a confined square cylinder. *J. Fluid Mech.*, 503:161–170, 2004.

J. Gerhard, M. Pastoor, R. King, B. R. Noack, A. Dillmann, M. Morzyński, and G. Tadmor. Model-based control of vortex shedding using low-dimensional Galerkin models. *AIAA-Paper* 2003-4262, *33rd AIAA Fluids Conference and Exhibit*, 2003.

W. R. Graham, J. Peraire, and K. Y. Tang. Optimal control of vortex shedding usind low-order models. Part I — Open-loop model development. *Int. J. Numer. Meth. Engrng.*, 44:945–972, 1999.

C. E. Grosch and H. Salwen. The continuous spectrum of the Orr-Sommerfeld equation. Part I. The spectrum and the eigenfunctions. *J. Fluid Mech.*, 87:33–54, 1978.

H. Haken. *Synergetics, An Introduction. Nonequilibrium Phase Transitions and Self-Organizations in Physics, Chemistry, and Biology.* Springer, New York, 3rd edition, 1983.

P. Holmes, J. L. Lumley, and G. Berkooz. *Turbulence, Coherent Structures, Dynamical Systems and Symmetry.* Cambridge University Press, Cambridge, 1st paperback edition, 1998.

C. John, B. R. Noack, M. Schlegel, F. Tröltzsch, and D. Wachsmuth. Optimal boundary control problems related to high lift configurations. In R. King, editor, *Active Flow Control II*, Notes on Numerical Fluid Mechanics and Multidisciplinary Design, Vol. 108, pages 405–419. Springer-Verlag, 2010.

B. H. Jørgensen, J. N. Sørensen, and M. Brøns. Low-dimensional modeling of a driven cavity flow with two free parameters. *Theoret. Comput. Fluid Dynamics*, 16:299–317, 2003.

D. D. Joseph. *Stability of Fluid Motions I & II.* Springer Tracts in Natural Philosophy - Vol. 26 & 27. Springer, Berlin, Heidelberg, New York, 1976.

C. Kasnakoglu, A. Serrani, and M. O. Efe. Control input separation by actuation mode expansion for flow control problems. *Internat. J. Control*, 81(9):1475–1492, 2008.

R. H. Kraichnan and S. Chen. Is there a statistical mechanics of turbulence? *Phys. D*, 37:160–172, 1989.

O. A. Ladyzhenskaya. *The Mathematical Theory of Viscous Incompressible Flow.* Gordon and Breach, New York, London, 1st edition, 1963.

L. D. Landau and E. M. Lifshitz. *Fluid Mechanics.* Course of Theoretical Physics, Vol. 6. Pergamon Press, Oxford, 2nd engl. edition, 1987.

O. Lehmann, M. Luchtenburg, B. R. Noack, R. King, M. Morzyński, and G. Tadmor. Wake stabilization using POD Galerkin models with interpolated modes. Invited Paper MoA15.2 of the *44th IEEE Conference on Decision and Control and European Control Conference ECC*, 2005.

M. Lesieur. *Turbulence in Fluids.* Kluwer Academic Publishers, Dordrecht, Boston, London, 2nd edition, 1993.

E. N. Lorenz. Deterministic nonperiodic flow. *J. Atm. Sci.*, 20:130–141, 1963.

D. M. Luchtenburg, B. Günter, B. R. Noack, R. King, and G. Tadmor. A generalized mean-field model of the natural and actuated flows around a high-lift configuration. *J. Fluid Mech.*, 623:283–316, 2009a.

D. M. Luchtenburg, B. R. Noack, and M. Schlegel. An introduction to the POD Galerkin method for fluid flows with analytical examples and MATLAB source codes. Technical Report 01/2009, Chair in Reduced-Order Modelling for Flow Control, Department of Fluid Dynamics and Engineering Acoustics, Berlin Institute of Technology, Germany, 2009b.

D. M. Luchtenburg, M. Schlegel, B. R. Noack, K. Aleksić, R. King, G. Tadmor, and B. Günther. Turbulence control based on reduced-order models and nonlinear control design. In R. King, editor, *Active Flow Control II*, Notes on Numerical Fluid Mechanics and Multidisciplinary Design, Vol. 108, pages 341–356. Springer-Verlag, 2010.

X. Ma and G. E. Karniadakis. A low-dimensional model for simulating three-dimensional cylinder flow. *J. Fluid Mech.*, 458:181–190, 2002.

J. Moehlis, T. R. Smith, P. Holmes, and H. Faisst. Models for turbulent plane Couette flow using the proper orthogonal decomposition. *Phys. Fluids*, 14:2493–2507, 2002.

A. S. Monin and A. M. Yaglom. *Statistical Fluid Mechanics I.* The MIT Press, Cambridge, Massachusetts, and London, 1971.

A. S. Monin and A. M. Yaglom. *Statistical Fluid Mechanics II.* The MIT Press, Cambridge, Massachusetts, and London, 1975.

M. Morzyński, W. Stankiewicz, B. R. Noack, F. Thiele, and G. Tadmor. Generalized mean-field model for flow control using continuous mode interpolation. Invited AIAA-Paper 2006-3488 of the *3rd AIAA Flow Control Conference*, 2006.

M. Morzyński, W. Stankiewicz, B. R. Noack, R. King, F. Thiele, and G. Tadmor. Continuous mode interpolation for control-oriented models of fluid flow. In R. King, editor, *Active Flow Control*, Notes on Numerical Fluid Mechanics and Multidisciplinary Design, Vol. 95, pages 260–278. Springer-Verlag, 2007.

B. R. Noack. *Niederdimensionale Galerkin-Modelle für laminare und transitionelle freie Scherströmungen (transl.: low-dimensional Galerkin models of laminar and transitional free shear flows).* Habilitation thesis, Berlin Institute of Technology, Germany, 2006.

B. R. Noack and H. Eckelmann. A global stability analysis of the steady and periodic cylinder wake. *J. Fluid Mech.*, 270:297–330, 1994a.

B. R. Noack and H. Eckelmann. A low-dimensional Galerkin method for the three-dimensional flow around a circular cylinder. *Phys. Fluids*, 6: 124–143, 1994b.

B. R. Noack, K. Afanasiev, M. Morzyński, G. Tadmor, and F. Thiele. A hierarchy of low-dimensional models for the transient and post-transient cylinder wake. *J. Fluid Mech.*, 497:335–363, 2003.

B. R. Noack, G. Tadmor, and M. Morzyński. Actuation models and dissipative control in empirical Galerkin models of fluid flows. Paper **FrP15.6** of the *The 2004 American Control Conference*, 2004.

B. R. Noack, P. Papas, and P. A. Monkewitz. The need for a pressure-term representation in empirical Galerkin models of incompressible shear flows. *J. Fluid Mech.*, 523:339–365, 2005.

B. R. Noack, M. Schlegel, B. Ahlborn, G. Mutschke, M. Morzyński, P. Comte, and G. Tadmor. A finite-time thermodynamics of unsteady fluid flows. *J. Non-Equilibr. Thermodyn.*, 33:103–148, 2008.

B. R. Noack, M. Schlegel, M. Morzyński, and G. Tadmor. System reduction strategy for Galerkin models of fluid flows. *Internat. J. Numer. Meth. Fluids*, 63(2), 231–248, 2010.

M. Pastoor, L. Henning, B. R. Noack, R. King, and G. Tadmor. Feedback shear layer control for bluff body drag reduction. *J. Fluid Mech.*, 608: 161–196, 2008.

B. Podvin. A proper-orthogonal-decomposition based for the wall layer of a turbulent channel flow. *Phys. Fluids*, 21:015111–1. . .18, 2009.

D. Rempfer. *Empirische Eigenfunktionen und Galerkin-Projektionen zur Beschreibung des laminar-turbulenten Grenzschichtumschlags (transl.: Empirical eigenfunctions and Galerkin projection for the description of the laminar-turbulent boundary-layer transition).* Habilitation thesis, Fakultät für Luft- und Raumfahrttechnik, Universität Stuttgart, 1995.

D. Rempfer. On low-dimensional Galerkin models for fluid flow. *Theoret. Comput. Fluid Dynamics*, 14:75–88, 2000.

D. Rempfer and F. H. Fasel. Dynamics of three-dimensional coherent structures in a flat-plate boundary-layer. *J. Fluid Mech.*, 275:257–283, 1994.

C. W. Rowley, I. Mezić, S. Bagheri, P. Schlatter and D.S. Henningson. Spectral analysis of nonlinear flows. *J. Fluid Mech*, 641:115–127, 2009.

B. Rummler. *Zur Lösung der instationären inkompressiblen Navier-Stokesschen Gleichungen in speziellen Gebieten (transl.: On the solution of the incompressible Navier-Stokes equations in some domains).* Habilitation thesis, Fakultät für Mathematik, Otto-von-Guericke-Universität Magdeburg, 2000.

H. Salwen and C. E. Grosch. The continuous spectrum of the Orr-Sommerfeld equation. Part 2. Eigenfunction expansions. *J. Fluid Mech.*, 104:445–465, 1981.

M. Schlegel, B. R. Noack, P. Comte, D. Kolomenskiy, K. Schneider, M. Farge, J. Scouten, D. M. Luchtenburg, and G. Tadmor. *Reduced-order*

modelling of turbulent jets for noise control, pages 3–27. In C. Brun, D. Juvé, M. Manhart, and C.-D. Munz, editors, *Numerical Simulation of Turbulent Flows and Noise Generation*, Notes on Numerical Fluid Mechanics and Multidisciplinary Design (NNFM), Vol. 104, pages 3–27. Springer-Verlag, 2009.

P. J. Schmid. Dynamic mode decomposition for numerical and experimental data. *J. Fluid. Mech* (in press), 2010.

S. G. Siegel, J. Seidel, C. Fagley, D. M. Luchtenburg, K. Cohen, and T. McLaughlin. Low dimensional modelling of a transient cylinder wake using double proper orthogonal decomposition. *J. Fluid Mech.*, 610:1–42, 2008.

L. Sirovich. Turbulence and the dynamics of coherent structures, Part I: Coherent structures. *Quart. Appl. Math.*, XLV:561–571, 1987.

G. Tadmor and B. R. Noack. Dynamic estimation for reduced Galerkin models of fluid flows. Paper **WeM18.1** of the *The 2004 American Control Conference*, 2004.

G. Tadmor, O. Lehmann, B. R. Noack, and M. Morzyński. Mean field representation of the the natural and actuated cylinder wake. *Phys. Fluids* 22 (3), 034102-1. . .22, 2010.

B. Thiria, S. Goujon-Durand, and J. E. Wesfreid. The wake of a cylinder performing rotary oscillations. *J. Fluid Mech.*, 560:123–147, 2006.

L. Ukeiley, L. Cordier, R. Manceau, J. Delville, J. P. Bonnet, and M. Glauser. Examination of large-scale structures in a turbulent plane mixing layer. Part 2. Dynamical systems model. *J. Fluid Mech.*, 441: 61–108, 2001.

M. Wei and C. W. Rowley. Low-dimensional models of a temporally evolving free shear layer. *J. Fluid Mech*, 618:113–134, 2009.

J. Weller, E. Lombardi, and A. Iollo. Robust model identification of actuated vortex wakes. *Physica D*, 238:416–427, 2009.